國 立 交 通 大 學

資訊科學與工程研究所

博 士 論 文

在WiMAX網路上的快速交遞協定設計與分析

Design and Analysis of Seamless Fast Handover Schemes for

WiMAX Networks

研 究 生：李龍昇

指導教授：王國禎　博士

中 華 民 國 一〇一 年 一 月

在WiMAX網路上的快速交遞協定設計與分析

Design and Analysis of Seamless Fast Handover Schemes for WiMAX Networks

研 究 生：李龍昇　　　　　　Student：Lung-Sheng Lee

指導教授：王國禎　　　　　　Advisor：Kuochen Wang

國 立 交 通 大 學

資 訊 科 學 與 工 程 研 究 所

博 士 論 文

A Dissertation

Submitted to Institutes of Computer Science and Engineering

Department of Computer Science

National Chiao Tung University

in Partial Fulfillment of the Requirements

for the Degree of

Doctor of Philosophy

in

Computer Science

January 2012

Hsinchu, Taiwan, Republic of China

中 華 民 國 一 〇 一 年 一 月

在WiMAX網路上的快速交遞協定設計與分析

學生：李龍昇　　指導教授：王國禎 博士

國立交通大學資訊科學與工程研究所

摘 要

　　本論文之目的是發展在WiMAX網路上無接縫快速交遞協定，以支援即時資料流及群播廣播(MBS)服務。IEEE 802.16e對即時資料流提供品質服務。然而在交遞過程中發生資料傳輸中斷仍是個待解決的重大課題，特別是在高速移動的行動裝置上所產生的頻繁交遞。因此，為提供即時資料流服務品質而設計一個可支援頻繁交遞及短暫服務中斷的交遞協定是必要的。在本論文中，我們提出一個符合IEEE 802.16e規範的新穎網路架構來支援無接縫的頻繁交遞，特別是支援高速移動的行動裝置。基於這個架構，我們提出一個在交遞過程中可以縮短服務中斷時間的網路輔助快速交遞(NFHO)協定。透過解決連線識別碼(CIDs)分配及上傳鏈結(uplink－UL)時序調整問題，我們提出的NFHO協定可以在交遞進行到ranging前，即可重啟上傳(UL)和下載(DL)資料，此點為本協定獨特的特色。我們同時發展一個分析模型，來探討交遞過程中的緩衝封包數目期望值(expected number of buffered packets)，封包遺失率(packet loss probability)，及服務中斷時間(service disruption time)。效能評估結果顯示，相較於IEEE 802.16e的硬式交遞協定，NFHO協定可降低75% DL服務中斷時間。另相較於Jiao et al.及IEEE

802.16e硬式交遞協定(Choi et al. 亦同)，NFHO協定可分別降低55.6%及75%的UL服務中斷時間。

此外，為了提供群播廣播服務，WiMAX標準制定在WiMAX網路上的資料傳輸協調機制。然而在此協調機制裡的封包遺失回復程序會增加封包傳輸延遲(packet transmission latency)及增大封包緩衝池(packet buffer pool)需求。在本論文中，我們提出一個in-frame control (IFC)機制來降低封包錯誤率(packet error rate)及封包重傳數(packet retransmission count)，此等同於降低封包傳輸延遲及封包緩衝池需求。此外，為支援level-2 frame-offset協調機制，我們提出一個可對任兩相鄰群播廣播服務區(MBS zones)間提供資料連續性服務的動態群播廣播服務區架構。基於此架構，我們提出一個無接縫的動態跨兩個群播廣播服務區之間的交遞協定(DMZ HO)來解決交遞時資料不連續(封包遺失)的問題。針對所提出的IFC機制，我們發展一個分析模型來分析封包錯誤率及封包重傳數。另針對DMZ HO，我們透過分析通道占用時間(channel occupation time)來評估所需額外頻寬(bandwidth overhead)。效能評估結果顯示，相較於制定在WIMAX標準中的原始機制，IFC機制可分別降低49.8% (error clusters arrival rate, $\lambda = 0.001$ (/ms))及49.73% ($\lambda = 0.001$ (/ms)) 的封包錯誤率及封包重傳數。除此之外，我們提出的DMZ HO機制，其效能勝過一個具有代表性的現有overlapping zone (OLZ)機制。相較於OLZ機制，當HO arrival rate為1 (/sec)時，DMZ HO機制可降低89.3%通道占用時間。 再則，我們提出的DMZ HO機制比OLZ機制消耗較少通道頻寬。DMZ HO機制的通道閒置率(channel idle ratio)是89.3% ($\mu = 1$, *PDU-offset* = 10) 遠大於同條件下的OLZ機制。

關鍵詞：IEEE 802.16e，快速交遞，封包遺失機率，服務中斷時間，frame-offset協調，群播廣播服務區，WiMAX

Design and Analysis of Seamless Fast Handover Schemes for WiMAX Networks

Student: Lung-Sheng Lee   Advisor: Dr. Kuochen Wang

Department of Computer Science
National Chiao Tung University

Abstract

The goal of this dissertation is to develop seamless fast handover schemes for supporting real-time traffic and multicast broadcast service (MBS) in WiMAX networks. The IEEE 802.16e provides QoS for real-time traffic; however, packet transmission disrupted by the handover (HO) process is still a big concern, especially when frequent HO is performed by mobile stations (MSs) with high mobility. Therefore, an HO scheme that supports frequent HO and also provides short service disruption time is necessary for providing QoS to real-time traffic. In this dissertation, we present a novel network architecture, which complies with the IEEE 802.16e standard, to support seamless frequent HO, especially for MSs with high mobility. Based on this architecture, a *network assisted fast handover* (NFHO) scheme is proposed to shorten service disruption time during the HO process. By resolving CIDs (connection identifiers) assignment and uplink timing adjustment issues, the proposed NFHO scheme can *restart both the uplink* (UL) and *downlink* (DL) *packet transmissions before the MS proceeds to the HO ranging*, which is a unique feature of our scheme. An analytic model has been developed to investigate the *expected number of buffered packets*, *packet loss probability*, and *service disruption time* during HO. Performance evaluation results show that the NFHO scheme reduces the DL service disruption time by 75% compared to the IEEE 802.16e hard HO scheme, and it also reduces the UL service disruption time by 55.6% and 75% compared to Jiao et al. and the IEEE 802.16e hard HO scheme (Choi et al. as well), respectively.

In addition, to support multicast broadcast service, the WiMAX standard defines a coordination mechanism to coordinate data transmission over the WiMAX network; however, the packet loss recovery procedures, which are parts of the coordination mechanism, enlarge the packet transmission latency and packet buffer pool requirement. In this dissertation, we propose an *in-frame control* (IFC) scheme to decrease the packet error rate and packet retransmission count, so as to reduce the packet transmission latency and packet buffer pool requirement. Furthermore, to support level-2 *frame-offset coordination*, we also propose a *dynamic MBS zone* (DMZ) framework that can provide data continuity between any two adjacent MBS zones. Based on the proposed DMZ framework, a seamless *dynamic inter-MBS zone handover* (called DMZ HO) scheme is proposed to resolve the data discontinuity (or packet loss) problem during inter-MBS zone HO. An analytic model has been developed to analyze the packet error rate and packet retransmission count for the proposed IFC scheme and the bandwidth overhead in terms of channel occupation time for the proposed DMZ HO. Performance evaluation results show that, compared to the original WiMAX scheme, defined in the WiMAX standard, the proposed IFC scheme reduces the packet error rate and packet retransmission count by 49.8% (error clusters arrival rate, $\lambda = 0.001$ (*/ms*)) and 49.73% ($\lambda = 0.001$ (*/ms*)), respectively. Moreover, the proposed DMZ HO scheme outperforms an existing overlapping zones (OLZ) scheme. It reduces channel occupation time by 89.3% compared to the OLZ scheme when the HO arrival rate, μ, is 1 (*/sec*). In addition, the proposed DMZ HO scheme consumes less channel bandwidth than the OLZ scheme. The channel idle ratio of the proposed DMZ HO scheme is 89.3% ($\mu = 1$, *PDU-offset* = 10) larger than that of the OLZ scheme.

Keywords: IEEE 802.16e, fast handover, packet loss probability, service disruption time, frame-offset coordination, MBS zone, WiMAX.

誌　謝

v

Contents

List of Figures

List of Tables

Chapter 1

Introduction

1.1 Background and Motivations

The IEEE 802.16-2004 standard was designed for rapid world wide deployment, cost-effectiveness and interoperable multi-vendor fixed broadband wireless access [1]. To support mobility service, based on the IEEE 802.16-2004, the IEEE 802.16e standard was designed to support mobile stations (MSs) moving at vehicle speeds [2]. The MAC layer handover (HO) process to support mobility between base stations (BSs) is provided. There are three layer-2 HO modes provided in the IEEE 802.16e. One is a hard HO mode and the others are two optional soft HO modes: Macro Diversity HO (MDHO) and Fast BS Switching (FBSS) [2]. An MS mandatorily supports the hard HO mode. There are several restrictions and extra hardware and software cost for the BSs to support MDHO or FBSS, such as synchronization on common time source, same frequency assignment and synchronized frame structure [2]. Therefore, the hard HO mode was adopted in most of existing IEEE 802.16e systems. The hard HO process consists of six stages: Cell Reselection, HO Decision and Initiation, Synchronization to Target BS Downlink, Ranging and Network Re-entry, Termination of MS Context, and HO Cancellation [2]. These stages can be functionally divided into two procedures: HO Preparation and HO Execution.

The HO Preparation procedure includes both Cell Reselection and HO Decision and Initiation stages. At the Cell Reselection stage, the MS requests the serving BS an allocation of

1

scanning intervals. After the serving BS grants the scanning intervals, the MS maintains current connections with the serving BS, and then scan and synchronize with neighboring (NBR) BSs to evaluate the quality of each channel. At the end of the Cell Reselection stage, the MS can obtain an availability list of NBR BSs. At the HO Decision and Initiation stage, an HO decision is made for the MS to HO from the serving BS to the target BS. The HO Execution procedure includes the following stages: Synchronization to Target BS Downlink, Ranging and Network Re-entry, Termination of MS Context, and HO Cancellation. In this procedure, the MS starts actual HO. The MS synchronizes to the downlink (DL) of the target BS and obtains uplink (UL) parameters. After completing the ranging process, the MS obtains new basic and primary management CIDs (connection identifiers), which will be used for transporting management messages, and adjusts UL parameters to synchronize to the UL. The MS then starts the Network Re-entry process that consists of Basic Capabilities Negotiation, Authorization, and Registration. In the registration of the Network Re-entry process, the target BS will reassign transport CIDs, which are used for transporting data packets, for active connections. After acquiring the transport CIDs, the MS is capable of starting data packet transmission. Termination of MS Context completes the HO process. In this stage, the serving BS releases the MS's context after the Resource Retain Timer expires. In addition, the HO Cancellation stage is used to handle the situation of the MS canceling the HO before the Resource Retain Timer expires.

In the HO Execution procedure, the data packet transmission is blocked until the MS acquires the transport CIDs in the registration of the Network Re-entry process. To reduce the packet transmission delay in the HO Execution procedure, the transport CIDs assignment and UL synchronization issues must be resolved in advance. Therefore, the objective of Chapter 3 is proposing an HO enhanced scheme which can resolve the transport CIDs assignment and UL synchronization issues ahead of the Ranging and Network Re-entry stage.

In addition, to support multicast and broadcast service (MBS) in the downlink, the IEEE 802.16-2009 provides macro-diversity and frame-level coordination modes among base stations (BSs) within an MBS zone. An MBS zone consists of a cluster of base stations (BSs) which transmit common MBS content with the same multicast connection identifier (MCID) and the same security association (SA). The backhaul MBS scheduler should coordinate all BSs within an MBS zone to synchronize MBS transmissions over radio interfaces. In an MBS zone, the set of medium access control (MAC) protocol data units (PDUs) carrying MBS content shall be identical in the same frame in all BSs [22]. To support intra-MBS zone data synchronization over radio interfaces, there are two options, macro-diversity and frame-level coordination, specified in the IEEE 802.16-2009 [22][23]. A macro-diversity MBS zone provides symbol level synchronization where the same MBS bursts are transmitted across involved BSs with time and frequency synchronized. An MBS zone, supporting frame-level coordination, provides frame-level synchronization, where the same MBS bursts are transmitted in the same frames across all involved BSs. In addition, to achieve MBS zone data synchronization, the WiMAX standard [23] defines a coordination mechanism to coordinate data transmission over the WiMAX network. The coordination mechanism includes a sync rule delivery procedure and recovery procedures. The sync rule delivery procedure announces the transmission timings of MBS bursts, and the recovery procedures consists of the sync rule recovery and the data path recovery, both of which are used to recover the lost sync rules and MBS payloads, respectively. The recovery procedures are based on the timeout and retransmission mechanisms. Because any packet error of MBS payloads or their associated sync rules should be recovered, it will results in long transmission latency and a large packet buffer pool requirement. An objective of Chapter 4 is proposing an in-frame control scheme to reduce the probability of entering recovery procedures so as to reduce packet transmission latency and packet buffer requirement.

For inter-MBS zone data synchronization, the WiMAX standard [23] defines level-1 and level-2 frame-offset coordination requirements. The level-1 frame-offset coordination provides service continuity, but it does not support data continuity; it only focuses on daisy-chaining of the MBS service flow, regardless of MBS data synchronization between two adjacent MBS zones. The level-2 frame-offset coordination is a more strict form of frame-offset coordination. From the transmission content perspective, the level-2 frame-offset coordination requirement is equivalent to the frame-level synchronization that provides data continuity service. In the level-2 frame-offset coordination, data continuity shall be maintained during inter-MBS zone HO. However, any two MBS zones might be served by different anchor ASN-GWs. The variances of packet transmission latencies from the CSN to the BSs of different MBS zones are big, and the coordination between anchor ASN-GWs for inter-MBS zone data synchronization is complicated. Therefore, supporting the level-2 frame-offset coordination shall be costly to achieve, especially when providing MBS service to a large geographic area. The other objective of Chapter 4 is proposing an inter-MBS zone HO scheme that can support the level-2 frame-offset coordination to maintain the continuity of data reception.

1.2 Contributions of the Dissertation

In this dissertation, we present seamless fast handover schemes to support real-time traffic and multicast broadcast service (MBS) in WiMAX networks. We also develop analytic models to evaluate the design approaches. The contributions of this dissertation are detailed as follows:

● We propose a network-assisted fast handover (NFHO) scheme to shorten the service disruption time during HO. By the proposed NFHO scheme, the UL/DL data transmission is able to be restarted before the MS proceeds to the HO ranging, which is a unique feature of our scheme. Experimental results show that the NFHO scheme reduces the DL service disruption time by 75% compared to the IEEE 802.16e hard HO scheme, and it also reduces

the UL service disruption time by 55.6% and 75% compared to Jiao et al. [15] and the IEEE 802.16e hard HO scheme (Choi et al.[14] as well), respectively. In summary, the proposed NFHO scheme has the best performance in terms of expected number of buffered packets, packet loss probability and service disruption time among existing hard HO schemes for the IEEE 802.16e.

- To reduce the probability of entering recovery procedures that enlarge packet transmission latency and packet buffer requirement, we propose an in-frame control (IFC) scheme that aggregates the MBS payload and its associated MBS sync rules. Performance evaluation results show that, compared to the original WiMAX scheme, the proposed IFC scheme reduces the packet error rate and packet retransmission count by 49.8% (error clusters arrival rate, $\lambda = 0.001$ (*/ms*)) and 49.73% ($\lambda = 0.001$ (*/ms*)), respectively.

- To support level-2 frame-offset coordination in WiMAX networks, we propose a seamless *dynamic inter-MBS zone handover* (called DMZ HO) scheme to resolve the data discontinuity (or packet loss) problem during inter-MBS zone HO. Performance evaluation results show that the proposed DMZ HO scheme outperforms an existing overlapping zones (OLZ) scheme [25]. It reduces channel occupation time by 89.3% compared to the OLZ scheme when the HO arrival rate, μ, is 1 (*/sec*). In addition, the proposed DMZ HO scheme consumes less channel bandwidth than the OLZ scheme. The channel idle ratio of the proposed DMZ HO scheme is 89.3% ($\mu = 1$, *PDU-offset* $= 10$) larger than that of the OLZ scheme.

1.3 Organization of the Dissertation

The rest of this dissertation is organized as follows. In Chapter 2, we survey the HO process in the IEEE 802.16e standard and review some existing IEEE 802.16e HO enhanced schemes. In addition, we survey the MBS data synchronization in the WiMAX standard and also review

some existing MBS zone HO schemes. In Chapter 3, the proposed network architecture and the proposed NFHO scheme are described. In addition, we develop an analytic model for performance evaluation. In Chapter 4, we describe the proposed DMZ HO scheme for inter-MBS zone HO. An analytic model is also developed for performance evaluation. In Chapter 5, we give some concluding remarks and future work.
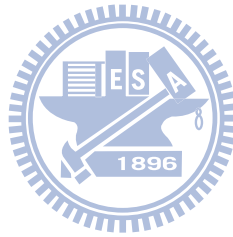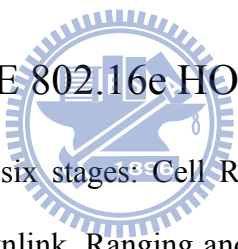
Chapter 2

Preliminaries and Related Work

In this Chapter, we survey the HO process in the IEEE 802.16e standard, and review existing IEEE 802.16e HO enhanced schemes. In addition, we brief the MBS data synchronization in the WiMAX standard [23] and review existing MBS zone HO schemes.

2.1 IEEE 802.16e HO Overview

2.1.1 Overview of the IEEE 802.16e HO Stages

The hard HO process consists of six stages: Cell Reselection, HO Decision and Initiation, Synchronization to Target BS Downlink, Ranging and Network Re-entry, Termination of MS Context, and HO Cancellation [2]. These stages can be functionally divided into two procedures: HO Preparation and HO Execution. The HO Preparation procedure includes both Cell Reselection and HO Decision and Initiation stages. At the Cell Reselection stage, the MS requests the serving BS an allocation of scanning intervals. After the serving BS grants the scanning intervals, the MS maintains current connections with the serving BS, and then scan and synchronize with neighboring (NBR) BSs to evaluate the quality of each channel. An initial ranging procedure which is termed as association here is processed during a scanning interval with one of NBR BSs. The association procedure can obtain service availability information and ranging parameters, both of which will be used for HO target selection and expedite the HO Execution procedure [2]. At the end of the Cell Reselection stage, the MS can obtain an

availability list of NBR BSs. At the HO Decision and Initiation stage, an HO decision is made for the MS to HO from the serving BS to the target BS.

The HO Execution procedure includes the following stages: Synchronization to Target BS Downlink, Ranging and Network Re-entry, Termination of MS Context, and HO Cancellation. In this procedure, the MS starts actual HO. The MS synchronizes to the downlink (DL) of the target BS and obtains uplink (UL) parameters. After completing the ranging process, the MS obtains new basic and primary management CIDs (connection identifiers), which will be used for transporting management messages, and adjusts UL parameters to synchronize to the UL. After synchronizing to the UL, the MS is capable of transmitting management messages. The MS then starts the Network Re-entry process that consists of Basic Capabilities Negotiation, Authorization, and Registration. Note that the ranging process in the Ranging and Network Re-entry stage is also termed as HO ranging. Moreover, in the registration of the Network Re-entry process, the target BS will reassign transport CIDs, which are used for transporting data packets, for active connections. After acquiring the transport CIDs, the MS is capable of starting data packet transmission. Termination of MS Context completes the HO process. In this stage, the serving BS releases the MS's context after the Resource Retain Timer expires. In addition, the HO Cancellation stage is used to handle the situation of the MS canceling the HO before the Resource Retain Timer expires. In the HO Execution procedure, the data packet transmission is blocked until the MS acquires the transport CIDs in the registration of the Network Re-entry process. Fig. 2.1 shows two packet disrupted periods in IEEE 802.16e hard HO process. To shorten the second packet disrupted period so as to reduce the packet transmission delay in the HO Execution procedure, the transport CIDs assignment and UL synchronization issues must be resolved in advance. Therefore, the objective of Chapter 3 is proposing an HO enhanced scheme which can resolve the transport CIDs assignment and UL synchronization issues ahead of the Ranging and Network Re-entry stage.
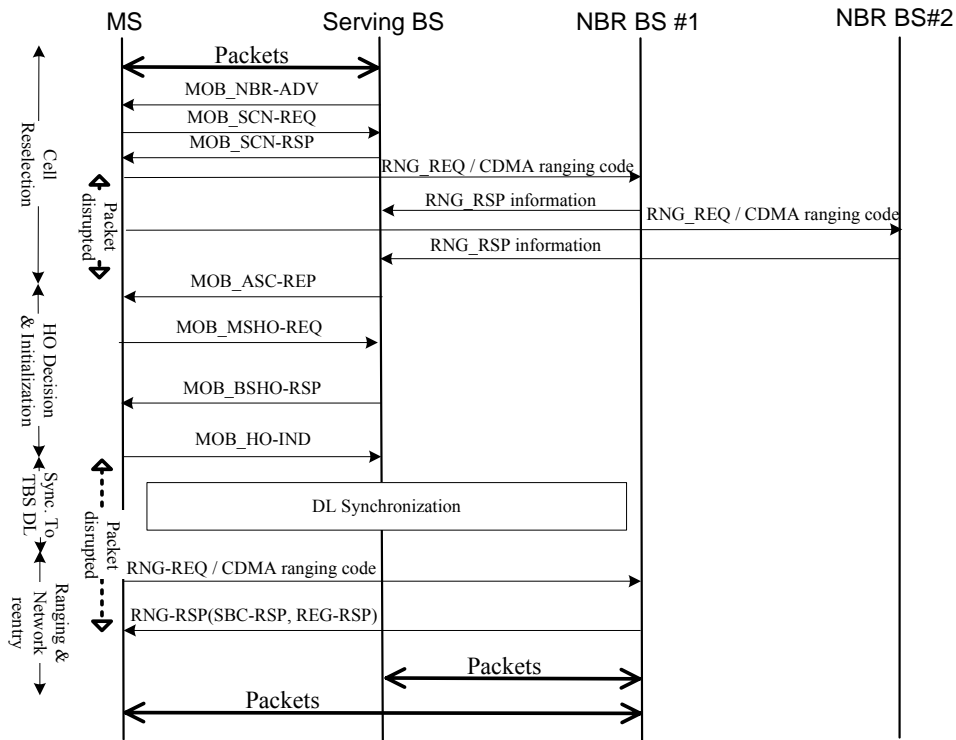
Fig. 2.1: Packet disruptions in IEEE 802.16e hard HO Process [2]

During the HO Execution procedure, the serving BS buffers incoming DL packets. Upon completion of network re-entry, the target BS, which now is the new serving BS, will forward the data packets received from the old serving BS to the MS. The HO process will prolong the packet transmission delay because data packets are held during the HO Preparation and Execution procedures. Shortening the service disruption time caused by the HO process will minimize the impact on QoS. In Chapter 3, we focus on the IEEE 802.16e hard HO mode and propose a novel network architecture for IEEE 802.16e networks. Based on the network architecture, we design a *network assisted fast handover* (NFHO) scheme to accelerate the HO Execution procedure and to reduce the service disruption time resulted from the Ranging and Network Re-entry stage. As mentioned above, the DL packets forwarding from the serving BS to the target BS will prolong the packet transmission delay, especially in frequent HO situations. The proposed NFHO scheme can reduce the DL packet forwarding delay by bicasting DL

packets to both the serving BS and target BS. It can also handle the problem of frequent HO of ping-pong mobility between BSs. An analytic model is developed to investigate the expected number of buffered packets, packet loss probability, and service disruption time during the HO Execution procedure. The analytic model is also used to analyze the performance among existing IEEE 802.16e HO enhanced schemes. We will show that the proposed NFHO scheme outperforms the existing IEEE 802.16e HO enhanced schemes. In addition, we will show that the packet loss probability is affected by the following network parameters: the HO service disruption time, the packet arrival rate of concurrent HO MSs, and the size of HO packet buffer pool. By the analytic model, we can evaluate the HO packet buffer pool utilization in a BS under different network parameter combinations and obtain a proper network parameter setting for meeting the QoS requirement. The analytic model can also be integrated to an admission control policy to provide proper QoS for incoming HO MSs.

2.1.2 IEEE 802.16e HO Scheme

In the IEEE 802.16e network, the BS periodically broadcasts network topology information via the MOB_NBR-ADV message. This message contains channel information of NBR BSs. Note that those message terms with all capital letters were defined in the IEEE 802.16e [2]. When an MS would like to HO, it starts the HO Preparation procedure and uses the MOB_SCN-REQ message to request a group of time intervals from the serving BS. Within the time intervals, the MS could seek and monitor a suitable BS from the list of candidate NBR BSs as the HO target. Following the MOB_SCN-RSP message, the MS starts scanning and attempts to synchronize with each NBR BS to evaluate the quality of the channel. During the scanning intervals, all incoming/outgoing packets to/from the MS shall be buffered until exiting the scanning mode and returning to the normal operation mode. The duration of a scanning interval depends on which level (2, 1 or 0) of the association procedure is chosen. With Network Assisted

Association Reporting (association level 2) [2], the MS will not wait for an RNG-RSP message from each NBR BS after sending a RNG-REQ message or CDMA ranging code (for OFDMA) to the NBR BS. Instead, each NBR BS will send the serving BS the RNG-RSP message over the backbone. All RNG-RSP messages from each NBR BS are finally collected in an MOB_ASC-REP message, which will be sent to the MS by the serving BS [2]. Therefore, association level 2 needs a shorter scanning interval than the other levels. When the MS decides to HO, an MOB_MSHO-REQ message will be sent to the serving BS. After negotiating with the selected target BS, the serving BS sends the MS an MOB_BSHO-RSP message that may include an Action Time parameter to specify when the target BS will allocate a Fast Ranging IE (Information Element) [2]. The MS could use the Fast Ranging IE to transmit the RNG-REQ message, which expedites the HO ranging. The MOB_HO-IND sent by the MS is used to commit the HO. After committing the HO to the serving BS, the MS enters the HO Execution procedure. The MS proceeds to synchronize with the DL and then performs HO ranging, UL parameters adjustment, basic capabilities negotiation, authorization, and registration with the target BS. During the HO Execution procedure, the serving BS holds data addressed to the MS, and the target BS may use RNG-RSP to notify the MS of DL data pending. Once the MS registers to the target BS successfully, the target BS starts transmitting the retained DL pending data, forwarded from the serving BS, to the MS. After the MS re-establishes IP connectivity and completes reception of DL pending data, the target BS then use a backbone message to request the old serving BS to stop forwarding DL data. Note that our proposed NFHO scheme can restart DL/UL data transmission before the HO ranging, which can greatly reduce the service disruption time. In section 3.1, we will detail the proposed NFHO scheme.

2.2 Related Work for Enhancing IEEE 802.16e HO

The HO of wireless networks can be classified into vertical HO and horizontal HO. An HO is defined as vertical if it occurs between heterogeneous wireless networks. The work in [3][4] proposes vertical HO decision algorithms to support HO between heterogeneous wireless networks. In contrast to vertical HO, an HO is defined as horizontal if it occurs between two adjacent cells of the same wireless network. In Chapter 3, we only focus on horizontal HO. Existing IEEE 802.16e horizontal HO enhanced schemes are reviewed in this section.

2.2.1 Existing IEEE 802.16e HO Enhanced Schemes

During the HO process, real-time services may be disrupted. As shown in Fig. 2.1, in the HO Preparation procedure, the MS stops normal data transmission for the scanning of NBR BSs, which results in the first packet disrupted period. And in the HO Execution procedure, the normal data transmission is blocked until the MS completes the Ranging and Network Re-entry stage, which results in the second packet disrupted period. The blocking of data transmission disrupts the service of real-time traffic and increases packet transmission delay that impacts the QoS provision.

Existing IEEE 802.16e HO enhanced schemes focus on either layer-3 or layer-2. Layer-3 HO schemes, such as [5]-[8], are basically based on the IEEE 802.16e layer-2 hard HO scheme to accelerate layer-3 HO for mobile IPv6, and they did not reduce the packet transmission delay on layer-2. Therefore, these layer-3 HO schemes also have at least the same service disruption time as the IEEE 802.16e hard HO scheme. Existing layer-2 HO enhanced schemes can be functionally classified into improvements on either the HO Preparation procedure or the HO Execution procedure. The work in [9]-[13] focused on the HO Preparation procedure, and their algorithms are to predict an HO target BS to reduce ping-pong effects and the number of NBR BS scanning. In addition to HO target BS prediction, [9] also proposed a fast synchronization

and association scheme that makes the MS be able to do data transmission with the serving BS and to do association with the target BS simultaneously. To realize this scheme, it would costly base on either MDHO or FBSS mode. In addition, wrong target BS estimation, due to the exhaustion of target BS resources and so on, may cause huge delay when the MS repeats to evaluate a next target BS candidate.

The studies in [14] and [15] focused on reducing data latency in the HO Execution procedure. In [14], the authors proposed a Fast_DL_MAP_IE message to restart DL data transmission before the MS proceeds to the Ranging and Network Re-entry stage. The target BS will use Fast_DL_MAP_IEs and old CIDs for transmitting DL data packets immediately after the MS completes the Synchronization to Target BS Downlink stage. After HO ranging is competed and the REG-RSP message, including new transport CIDs assignment for active connections, is received, the MS will return to use normal DL_MAP_IE with new assigned transport CIDs. Similar to [14], the authors in [15] proposed another Transport CIDs assignment scheme to restart DL data transmission before the MS proceeds to the Ranging and Network Re-entry stage. Through its transport CIDs assignment scheme, the target BS can use the old transport CIDs, which were used in the serving BS, to transmit DL packets with no CID conflicts between the serving BS and the target BS. The MS uses old transport CIDs until it receives the REG-RSP message, which assigns new transport CIDs to active connections. Both schemes in [14] and [15] restart DL data transmission before the MS proceeds to the HO ranging; however, this feature is not applicable to the UL real-time traffic of these two schemes. This is because the scheme in [14] did not provide mechanisms to pre-acquire UL synchronization parameters, which is acquired during HO ranging, and new transport CIDs, which is acquired during registration. As to the scheme in [15], it can use old transport CIDs for UL data transmission until it receives the REG-RSP message; however, it did not provide mechanisms to pre-acquire

UL synchronization parameters. Thus, the scheme in [15] can advance UL data transmission only after HO ranging.

To restart UL data transmission, the MS should synchronize to the UL first. Since the RNG-RSP message provides UL synchronization parameters, such as frequency corrections, transmission power level corrections, UL timing offset corrections, and basic and primary management CIDs assignment, to advance UL data transmission, the UL parameters should be obtained ahead of schedule. In Chapter 3, we focus on reducing the service disruption time during the HO Execution procedure and propose an NFHO scheme that can restart both DL and UL data transmissions before the MS proceeds to the HO ranging. We will detail our scheme in section 3.1.

2.2.2 Qualitative Comparison of Existing IEEE 802.16e HO Enhanced Schemes
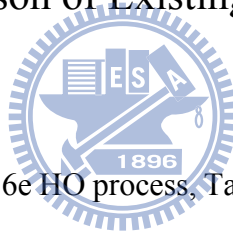
Focusing on the layer-2 IEEE 802.16e HO process, Table 2.1 shows a qualitative comparison of the existing IEEE 802.16e HO enhanced schemes. As mentioned above, existing layer-3 schemes were all based on the IEEE 802.16e layer-2 hard HO scheme. Therefore, from the layer-2 view, we regard the layer-3 schemes as the same as the IEEE 802.16e hard HO scheme. Lee. et al. [9] is a representative of those schemes that focus on improving the HO Preparation procedure. Choi et al. [14] and Jiao et al. [15] focus on the HO Execution procedure, which is also the focus of the proposed NFHO scheme. Among existing IEEE 802.16e HO enhanced schemes, [15] is the only paper that dealt with the reduction of both DL and UL data latencies. Our proposed NFHO scheme is also included in this qualitative comparison. Note that, to the best of our knowledge, our scheme is the only scheme that can restart data transmission at both DL and UL before the MS proceeds to the HO ranging.

Table 2.1: Comparison among existing IEEE 802.16e HO schemes.

Scheme	Improvement on / design focus	Data transmission restarts at	CID_Update required
Association level 2 of 802.16e [2]	HO Preparation procedure/ Reduce NBR BS association time	DL/UL after REG-RSP	Yes
Lee et al. [9]	HO Preparation procedure / 1. Reduce the number of NBR BSs scanning 2. Reduce association time	DL/UL after REG-RSP	Yes
Choi et al. [14]	HO Execution procedure / Reduce DL data latency	1. DL before HO ranging 2. UL after REG-RSP	Yes
Jiao et al. [15]	HO Execution procedure / Momentarily reuse old CIDs to reduce DL and UL data latency	1. DL before HO ranging 2. UL after HO ranging	Yes
NFHO (Proposed)	HO Execution procedure / 1. Fast UL synchronization 2. Reduce DL and UL data latency	DL/UL before HO ranging	Intra-CSSC HO: No Inter-CSSC HO: Yes

2.3 MBS in WiMAX Networks

2.3.1 WiMAX Standard for MBS

To concurrently transport common data to a group of mobile stations (MSs), the IEEE 802.16-2009 introduces multicast and broadcast service (MBS) in the downlink and provides macro-diversity and frame-level coordination modes among base stations (BSs) within an MBS zone. An MBS zone consists of a cluster of base stations (BSs) which transmit common MBS content with the same multicast connection identifier (MCID) and the same security association (SA). The backhaul MBS scheduler should coordinate all BSs within an MBS zone to synchronize MBS transmissions over radio interfaces. In an MBS zone, the set of medium access control (MAC) protocol data units (PDUs) carrying MBS content shall be identical in the same frame in all BSs [22]. To support intra-MBS zone data synchronization over radio interfaces, there are two options, macro-diversity and frame-level coordination, specified in the IEEE 802.16-2009 [22][23]. A macro-diversity MBS zone provides symbol level synchronization where the same MBS bursts are transmitted across involved BSs with time and frequency synchronized. An MBS zone, supporting frame-level coordination, provides frame-level synchronization, where the same MBS bursts are transmitted in the same frames across all involved BSs. In addition, to achieve MBS zone data synchronization, the WiMAX standard [23] defines a coordination mechanism to coordinate data transmission over the WiMAX network. The coordination mechanism includes a sync rule delivery procedure and recovery procedures. The sync rule delivery procedure announces the transmission timings of MBS bursts, and the recovery procedures consists of the sync rule recovery and the data path recovery, both of which are used to recover the lost sync rules and MBS payloads, respectively. An MBS payload, including an MBS datagram, carries MBS content. The recovery procedures are based on the timeout and retransmission mechanisms.

In Chapter 4, we propose an in-frame control (IFC) scheme that aggregates MBS payloads and their associated sync rules. By this scheme, we can reduce the probability of entering recovery procedures so as to reduce packet transmission latency and packet buffer requirement. In addition, to maintain maximum service continuity during inter-MBS zone HO, the WiMAX standard [23] defines a *frame-offset coordination* requirement for inter-MBS zone data synchronization. The frame-offset coordination defines that the same MBS service flow transmitted in any two adjacent MBS zones should be restricted to a specified number of frame-offset boundary [23]. The specified number of frame-offset boundary should be restricted within 7 frames [22][23]. Two levels of coordination requirements were defined. The level-1 coordination and level-2 coordination require service continuity and data continuity, respectively, between any two adjacent MBS zones. The service continuity focuses on providing non-interruption MBS service regardless of data discontinuity. The data continuity is a more strict form of service continuity; it provides not only service continuity but also non-interrupted MBS data reception. Consequently, from a data content perspective, the level-2 frame-offset coordination is the same with the frame-level coordination [23] , which provides HO MSs with data continuity during intra-MBS zone HO. In two adjacent MBS zones, one MBS zone may transmit a specific MBS MAC PDU earlier or later than the other MBS zone. In this dissertation, the offset in units of MBS MAC PDU between two adjacent MBS zones is termed as PDU-offset (PDU-O), and the MBS MAC PDUs involved in the offset are termed as PDU-O packets. The PDU-O shall be zero if the same MBS MAC PDU is transmitted across two adjacent MBS zones with frame synchronized. A positive PDU-O value will result in packet loss during inter-MBS zone HO because the MS handovers to the target MBS zone that has transmitted the next expected MBS PDU earlier than the source MBS zone. A positive PDU-O value is the number of lost packets during the inter-MBS zone HO. A negative PDU-O value implies that the MS will receive redundant packets immediately from the target MBS zone right after HO. For data

continuity requirement of the level-2 frame-offset coordination, the packet loss should be resolved during inter-MBS zone HO. To support level-2 frame-offset coordination, we propose a dynamic MBS zone (DMZ) framework that can provide seamless HO between any two adjacent MBS zones. Based on this framework, we then propose a DMZ HO scheme to resolve the positive PDU-O value problem so as to provide data continuity during inter-MBS zone HO.

2.3.2 MBS Data Synchronization

To provide seamless HO without interrupting MBS service, the WiMAX backhaul network shall synchronize MBS data transmissions between BSs. Fig. 2.2 shows the network reference model of the WiMAX network [23]. The connectivity service network (CSN) provides IP connectivity service and authentication, authorization and accounting (AAA) functions to MSs. The access service network gateway (ASN-GW) connecting to a CSN provides handover relay, control path and data path functions. A set of BSs, providing HO and radio resource management, are linked to an ASN-GW.
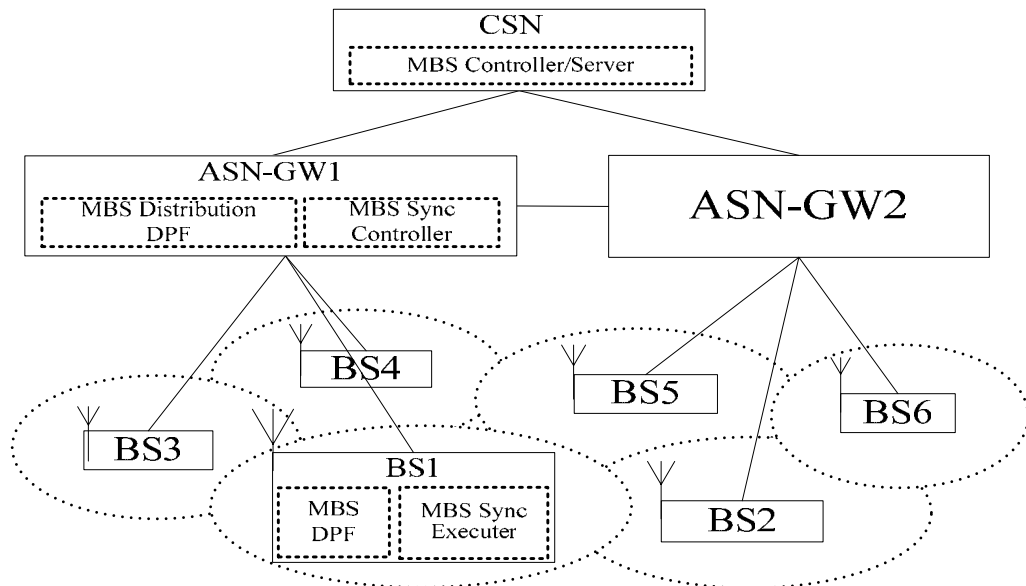
Fig. 2.2: WiMAX network framework and functional components [23].

To provide MBS service, some MBS functional components are defined in the WiMAX network. The MBS controller/server performs IP multicast group management, MBS program management, and MBS service announcement. The MBS distribution DPF (data path function) and MBS DPF handle the bearer control management. The MBS sync controller and MBS sync executer are designed to synchronize downlink transmission in one or more MBS zones. The MBS sync controller coordinates radio resources of the BSs and retrieves MBS data for scheduling MBS bursts. It determines the mappings from MBS protocol data units (PDUs) to MBS bursts. Then, the parameters of each MBS burst are delivered to the BSs belonging to the same MBS zone in the form of MBS sync rule announcement packets, which is abbreviated to sync rules. [23]. By this way, the MBS sync controller uses centralized control to synchronize MBS bursts among the BSs in the same MBS zone. Note that an MBS zone is only synchronized by an MBS sync controller; however, an MBS sync controller may coordinate more than one MBS zone [23].
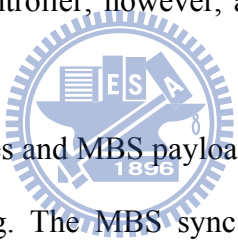
After receiving MBS sync rules and MBS payloads, the MBS sync executer handles MBS bursts constructing and scheduling. The MBS sync rule carries the next sync rule arrival timestamp information so that the MBS sync executer can start the sync rule recovery procedure if the next MBS sync rule was not received at the expected timestamp. Three time periods are defined for transmission synchronization. The Accumulation Period accumulates MBS payloads, and the following Recovery Period recovers lost payloads during the Accumulation Period. The final Transmission Period starts MBS bursts transmission. The MBS DPF shall start the data recovery procedure if detecting packet loss by checking generic routing encapsulation (GRE) sequence numbers of the received MBS payloads. Therefore, for transmission synchronization, the WiMAX standard [23] assumes that the MBS services are delay tolerant.

To achieve the frame-level synchronization requirement, the WiMAX standard [23] uses a centralized MBS Sync Controller and an MBS Distribution DPF to send the MBS sync rules and

MBS payloads, respectively, to all BSs in the same MBS zone. Therefore, the MBS data content shall be the same in the same frame in all BSs in the same MBS zone [23]. The ASN-GW which coordinates data synchronization in an MBS zone is termed as an anchor ASN-GW.

For inter-MBS zone data synchronization, the WiMAX standard [23] defines level-1 and level-2 frame-offset coordination requirements. For inter-MBS zone HO MSs, the level-1 frame-offset coordination provides service continuity, but it does not support data continuity; it only focuses on daisy-chaining of the MBS service flow, regardless of MBS data synchronization between two adjacent MBS zones. The level-2 frame-offset coordination is a more strict form of frame-offset coordination; it requires the data transmissions between any two adjacent MBS zones are synchronized so that it can provide HO MSs with data continuity during inter-MBS zone HO [23]. Therefore, during inter-MBS zone HO, supporting data continuity for HO MSs is equivalent to support the level-2 frame-offset coordination. From the transmission content perspective, the level-2 frame-offset coordination requirement is equivalent to the frame-level synchronization that provides data continuity service for intra-MBS zone HO MSs [23]. To support the level-2 frame-offset coordination, we should maintain data continuity during inter-MBS zone HO. However, any two MBS zones might be served by different anchor ASN-GWs. The variances of packet transmission latencies from the CSN to the BSs of different MBS zones are big, and the coordination between anchor ASN-GWs for inter-MBS zone data synchronization is complicated. Therefore, supporting the level-2 frame-offset coordination shall be costly to achieve, especially when providing MBS service to a large geographic area. In Chapter 4, we propose a dynamic MBS zone framework to support the level-2 frame-offset coordination and to maintain data continuity for inter-MBS zone HO. The proposed framework only coordinates any two adjacent MBS zones; therefore, it can easily support MBS service in a large geographic area. We will detail this in section 4.1.

TABLE 2.2: COMPARISON OF EXISTING INTER-MBS ZONE HO SCHEMES.

Scheme	Design focus / Improvements	Packet loss / Data continuity maintained	Bandwidth overhead
Original WiMAX scheme [23]	Use daisy-chaining of MBS MAP [1] to support level-1 coordination / Maintain service continuity	Yes / No	No
LMA [24]	Enlarge zones to reduce inter-zone HO probability / Reduce HO delay	Yes / No	No
OLZ [25]	Use static overlapping zones to avoid inter-zone HO / 1. Reduce HO delay 2. Data continuity not addressed in [25]	(not addressed in [25])	Large
DMZ HO (Proposed)	Use dynamic overlapping zones to resolve data discontinuity / 1. Reduce HO delay 2. Maintain data continuity	No / Yes	Small

2.4 Related Work for Enhancing Inter-MBS HO

During inter-MBS zone HO, the MBS services may be disrupted. The service disruption may be resulted from the HO delay and the data discontinuity between source and target MBS zones. In the IEEE 802.16-2009 [1], it supports daisy-chaining of MBS MAP messages that can be applied to support the level-1 frame-offset coordination. In Chapter 4, the daisy-chaining scheme for inter-MBS zone HO is termed as the original WiMAX scheme [23]. In [24], the authors reduce the average inter-MBS zone HO delay by reducing the possibility of inter-MBS zone HO. An MBS zone is partitioned into multiple location management areas (LMAs). By tracking the locations of MBS users, the packets are only selectively transmitted to LMAs in which the MBS users reside. As a result of saving radio bandwidth in those LMAs in which no any MBS user resides, the LMA scheme [24] allows a large MBS zone configuration that can reduce the number of inter-MBS zone HOs. The LMA scheme focuses on inter-MBS zone HO avoidance instead of focusing on data continuity and packet loss issues during inter-MBS zone HO. The study in [25] focuses on reducing the inter-MBS zone HO delay by using an overlapping zone (OLZ) configuration. The OLZ scheme [25] configures the overlapped area between any two adjacent MBS zones in a cell. Therefore, a cell overlapped by three adjacent MBS zones uses triple bandwidth to send the same MBS service. When an MBS user moves to a cell with overlapped zones, the MBS user also joins all overlapped MBS zones belonging to the same MBS service. The OLZ scheme focuses on reducing the HO delay and avoiding inter-MBS zone HO. However, it results in large bandwidth overhead, especially in a cell overlapped by three adjacent MBS zones.

In Chapter 4, we propose a *dynamic MBS zone* (DMZ) framework to support the level-2 frame-offset coordination. Based on the proposed DMZ framework, a seamless *dynamic inter-MBS zone handover* (called DMZ HO) scheme is proposed to resolve the data discontinuity (or packet loss) problem during inter-MBS zone HO. In section 4.1, we will detail

the proposed DMZ HO. Table 2.2 shows a qualitative comparison of the existing inter-MBS zone HO schemes. Note that the proposed DMZ HO scheme is also included for comparison. Note that the proposed DMZ HO scheme, using dynamic overlapping zones, is much more cost-effective than the OLZ scheme [25], which uses static overlapping zones and has large bandwidth overhead.
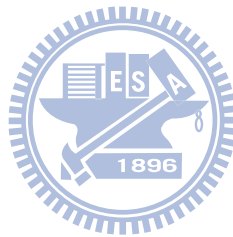
Chapter 3

A Network Assisted Fast Handover Scheme for IEEE 802.16e Networks

In this Chapter, we present a novel network architecture, which complies with the IEEE 802.16e standard, to support seamless frequent HO, especially for MSs with high mobility. Based on this architecture, a *network assisted fast handover* (NFHO) scheme is proposed to shorten service disruption time during the HO process. By resolving CIDs (connection identifiers) assignment and uplink timing adjustment issues, the proposed NFHO scheme can *restart both the uplink* (UL) and *downlink* (DL) *packet transmissions before the MS proceeds to the HO ranging*, which is a unique feature of our scheme. In addition, based on the NFHO scheme, an analytic model has been developed to investigate the *expected number of buffered packets*, *packet loss probability*, and *service disruption time* during HO. Performance evaluation results show that the NFHO scheme reduces the DL service disruption time by 75% compared to the IEEE 802.16e hard HO scheme, and it also reduces the UL service disruption time by 55.6% and 75% compared to Jiao et al. and the IEEE 802.16e hard HO scheme (Choi et al. as well), respectively. In addition, the proposed NFHO scheme has the best performance in terms of expected number of buffered packets and packet loss probability among existing hard HO schemes for the IEEE 802.16e. Furthermore, our analytic model can be integrated to an admission control policy to guarantee proper QoS for ongoing HO MSs.

3.1 Proposed NFHO Scheme

To restart data transmission ahead of the Ranging and Network Re-entry stage, two issues need to be resolved. One is UL synchronization and the other is updating transport CIDs, which are used by active connections for data transmission in the target BS. We first propose a novel network architecture for IEEE 802.16e networks. Based on this architecture, a network-assisted fast HO (NFHO) scheme is proposed to reduce the execution time of the HO Execution procedure. Fig. 3.1 shows the proposed network architecture. A set of BSs are linked to a convergence sublayer switch center (CSSC) through the wired network. Here we design a CSSC that handles two original CS functions: the MAC function of the service-specific CS (either ATM CS or packet CS) and the backbone management messages exchange. In addition, the CSSC also handles control messages for bicasting data packets to both the serving BS and the selected target BS. A BS handles the functions of MAC CPS, security sublayer, and PHY layer.
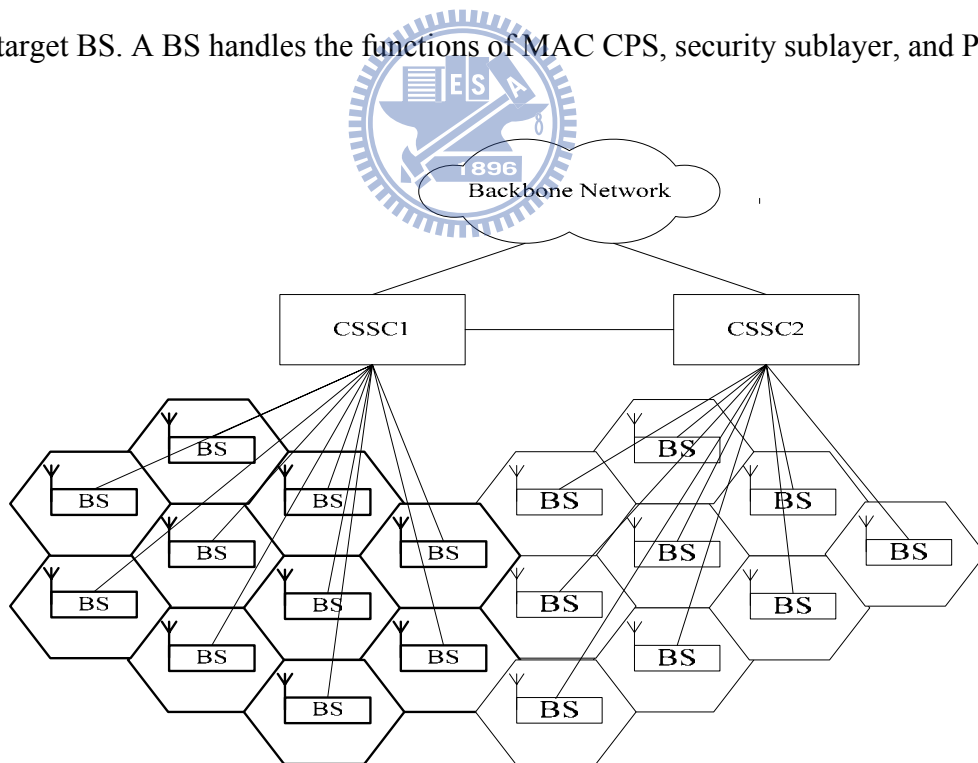
Fig. 3.1: Proposed network architecture for IEEE 802.16e networks.
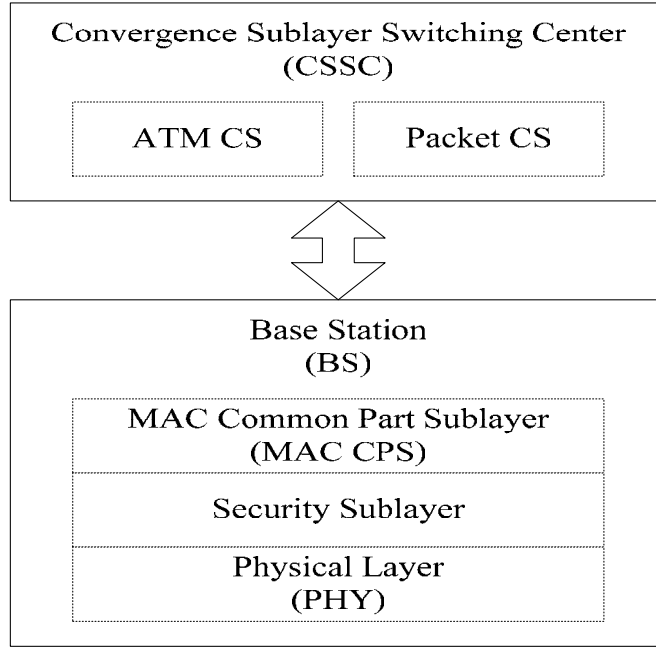
Fig. 3.2: Protocol layering of the proposed network architecture.

Fig. 3.2 illustrates the protocol layering of the proposed network architecture. We place ATM CS and packet CS in the CSSC. The HO within a CSSC is termed as *intra-CSSC HO*, and the HO between CSSCs is termed as *inter-CSSC HO*. The CIDs need to be changed only when the MS handovers to a BS that belongs to another CSSC. That is, based on the proposed network architecture, the target BS does not need to reassign CIDs for intra-CSSC HO. To reassign CIDs for inter-CSSC HO, we propose control messages, exchanged between serving BS and target BS in the HO Decision and Initialization stage, to pre-assign CIDs for the MS. Therefore, the MS can obtain new CIDs before entering the HO Execution procedure. In this way, the CIDs reassignment issue can be resolved. The control messages exchange for CID pre-assignment during inter-CSSC HO will be detailed in section 3.1.2.

To resolve UL synchronization, we propose to redo association level 2 in the HO Decision and Initialization stage. After a target BS is selected, the MS may redo scanning and association level 2 for the selected target BS if the current UL synchronization parameters obtained from the Cell Reselection stage are considered not up-to-date. Therefore, the MS can obtain correct UL synchronization parameters before entering the HO Execution procedure. After synchronizing to

the DL in the Synchronization to Target BS Downlink stage, the MS can adjust the UL synchronization parameters to synchronize to the UL immediately. Besides, we also propose an open-loop fine-tuning method that can improve the accuracy of the UL timing adjustment offset. The open-loop fine-tuning method is detailed in section 3.1.1.

We use the same CIDs and the pre-assigned CIDs for intra-CSSC HO and inter-CSSC HO, respectively. Furthermore, the proposed scheme enables the MS to synchronize to the UL immediately after the DL is synchronized. Since DL packets are bicast to the selected target BS as well as the serving BS at the HO Decision and Initialization stage, the transmission of both DL and UL packets can be immediately restarted after the MS completes the Synchronization to Target BS Downlink stage. Therefore, we can shorten the packet transmission delay resulted from waiting for the completion of the Ranging and Network Re-entry stage during the HO Execution procedure. The detailed intra-CSSC HO and inter-CSSC HO message sequence charts (MSCs) are described in the section 3.1.2.

Note that the proposed network architecture complies with the IEEE 802.16e standard. Since the CSSC still handles its original CS functions, it can follow MAC SAP specifications to access the MAC CPS. As to the backbone management messages, exchanging between CSSC and MAC CPS, can be handled by an add-on software component for supporting the proposed NFHO scheme. That is, only an add-on software component with a small cost is required to support the proposed NFHO scheme. Note that even without the add-on software component, the CSSC and BS can still function through the MAC SAP for supporting the original IEEE 802.16e hard HO scheme. Therefore, the proposed network architecture complies with the IEEE 802.16e standard. Note that in the proposed network architecture, the CSSC is logically separated as an individual component; however, from an implementation perspective, the CSSC can be still located in one of the BSs, and the other BSs have wired links to the CSSC.
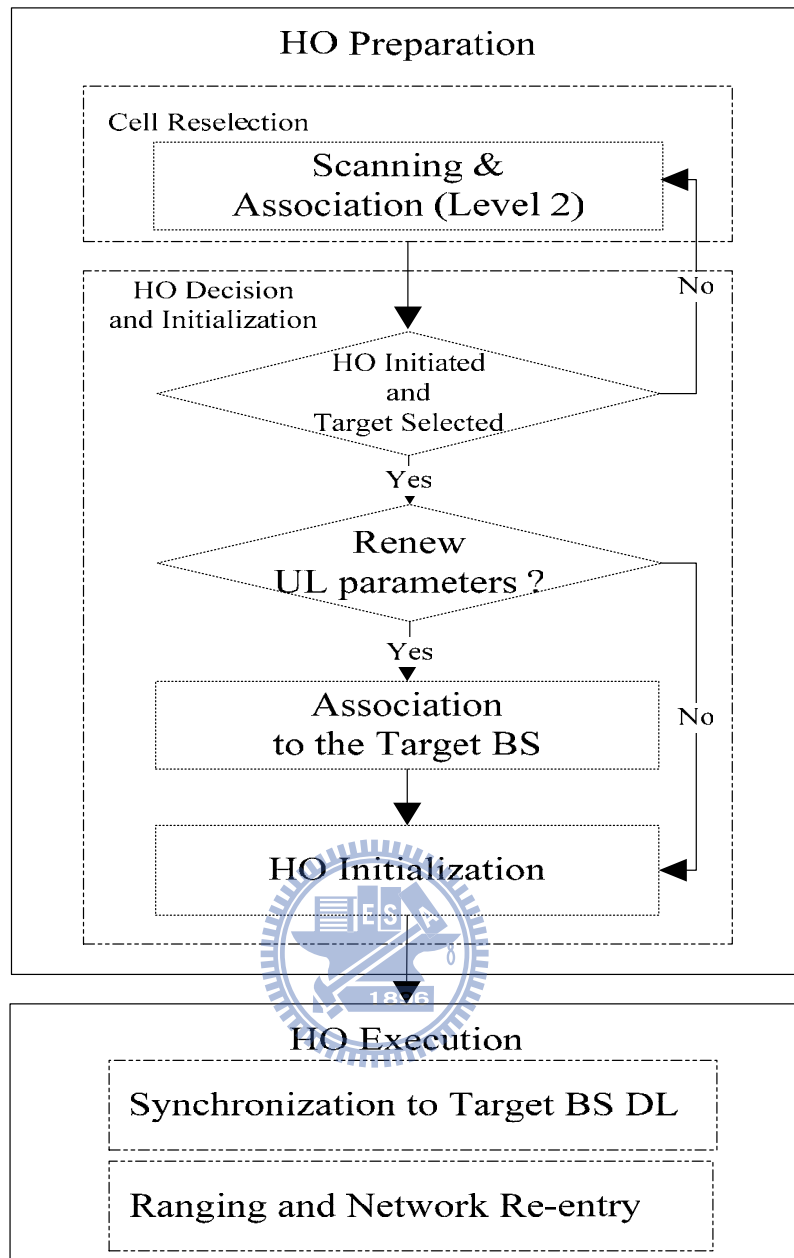
Fig. 3.3: Re-association to renew UL parameters.

3.1.1 Acquiring UL Synchronization Parameters

Association in the Cell Reselection stage is used to acquire ranging parameters and service availability information that could expedite the HO Execution procedure. In the IEEE 802.16e, association level 2 provides better efficiency than the other two association levels (0 and 1). Here we assume association level 2 is adopted. As mentioned above, after an HO target BS is selected, we redo association to acquire fresh UL synchronization parameters in the HO

Decision and Initiation stage. Fig. 3.3 shows the flow chart of re-association to the selected target BS for acquiring UL synchronization parameters. If the UL parameters of the selected target BS are considered to be out-of-date, the MS should renew the UL parameters by doing association to the selected target BS. The decision to renew UL parameters depends on some factors, such as the difference of DL arrival times since last association, the decay of mean CINR (carrier to interference and noise ratio) since last association, and a refresh timer. Here we simply assume that the MS decides to renew the UL parameters when a refresh timer has expired.
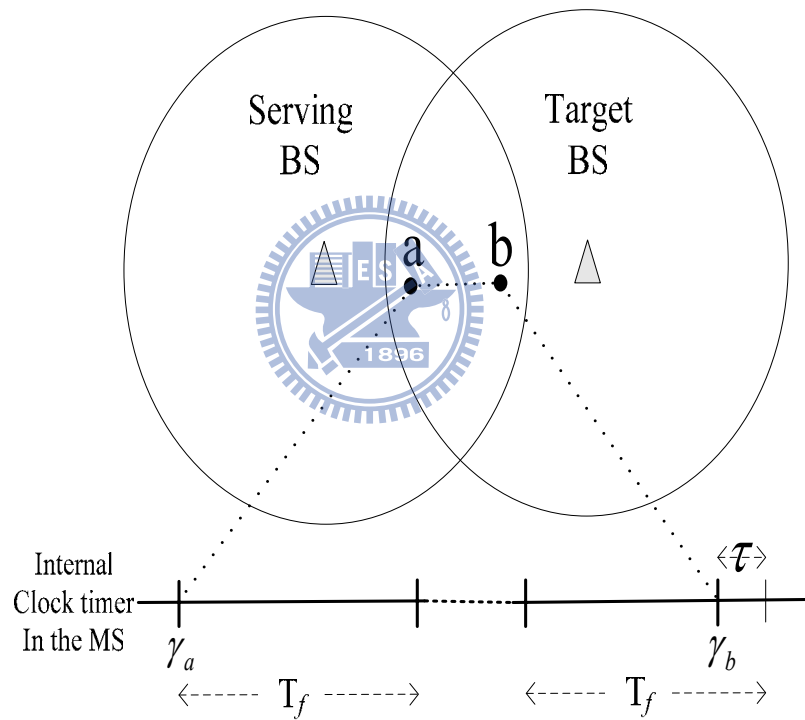
Fig. 3.4: The difference of DL signal delays between synchronization at the association and synchronization at the Synchronization to Target BS DL stage.

Based on the difference of DL signal delays between the synchronization at the association and the synchronization at the Synchronization to Target BS DL stage, we propose an open-loop fine-tuning method to acquire a correct UL timing adjustment offset. Fig. 3.4 shows the difference of DL signal delays between locations 'a' and 'b'. The MS did association with the

target BS at location 'a', and a frame was synchronized at γ_a, which was the clock time measured by the MS. During the Synchronization to Target BS DL stage, the MS moves to location 'b', and a frame is synchronized at γ_b, which is the clock time measured by the MS. Therefore, we have

$$\gamma_b - \gamma_a = n \cdot T_f + \tau , \quad |\tau| << T_f ,$$

where T_f is the frame duration, n is the number of frames in the time period between 'a' and 'b', and τ is the difference of DL signal delays between locations 'a' and 'b'. Since the UL has also the same difference of the UL signal delays between 'a' and 'b' as that of the DL, we add the difference, τ, to fine-tune the UL timing adjustment offset. Thus, we have

$$\eta_b = \eta_a + \tau$$

where η_a is the UL timing adjustment offset obtained from the last association, and η_b is the fine-tuned UL timing adjustment offset that will be used at the Synchronization to Target BS Downlink stage. By acquiring a correct UL timing adjustment offset, the MS can also synchronize to the UL immediately after synchronizing to the DL of the target BS. As a result, the MS can restart the DL and UL data transmissions before the Ranging and Network Re-entry stage.

3.1.2 Fast HO Execution Procedure with QoS Support

To reduce the packet transmission delay due to the HO Execution procedure, based on our proposed network architecture, we bicast DL traffic to both the serving BS and the selected target BS to avoid the latency caused by data forwarding. Note that bicasting DL traffic will incur extra bandwidth overhead between CSSC and BS. However, since the link between CSSC and BS is a wired link, the extra bandwidth overhead is not a concern. In the HO Execution procedure of the IEEE 802.16e, the UL/DL data packets can only be transmitted after the Ranging and Network Re-entry stage. In the Ranging and Network Re-entry stage, the IEEE

802.16e provides HO optimization options that could omit authorization by sharing the MS's context between the serving BS and target BS and grouping the Basic Capabilities Negotiation and Registration into the HO ranging. Note that the configuration of the HO optimization options in each BS shall be announced in the MOB_NBR-ADV message. Therefore, by configuring the HO optimization options, data transmission could be restarted immediately after the HO ranging. In the HO ranging, the target BS provides the MS necessary parameters, including UL timing adjustment offset, frequency corrections, transmission power level corrections, and basic and primary management CIDs. The proposed NFHO scheme shortens the data transmission delay by restarting the UL and DL data transmissions ahead of the HO ranging. Remind that these parameters, except basic and primary management CIDs, can be obtained in the last association, and the UL timing adjustment offset can be further fine-tuned for UL synchronization in the Synchronization to Target BS Downlink stage. In addition, based on the proposed network architecture, the intra-CSSC HO does not need to update transport CIDs. Therefore, normal data packet transmission can be restarted before the HO ranging, and the service disruption time resulted from the HO ranging could be eliminated.
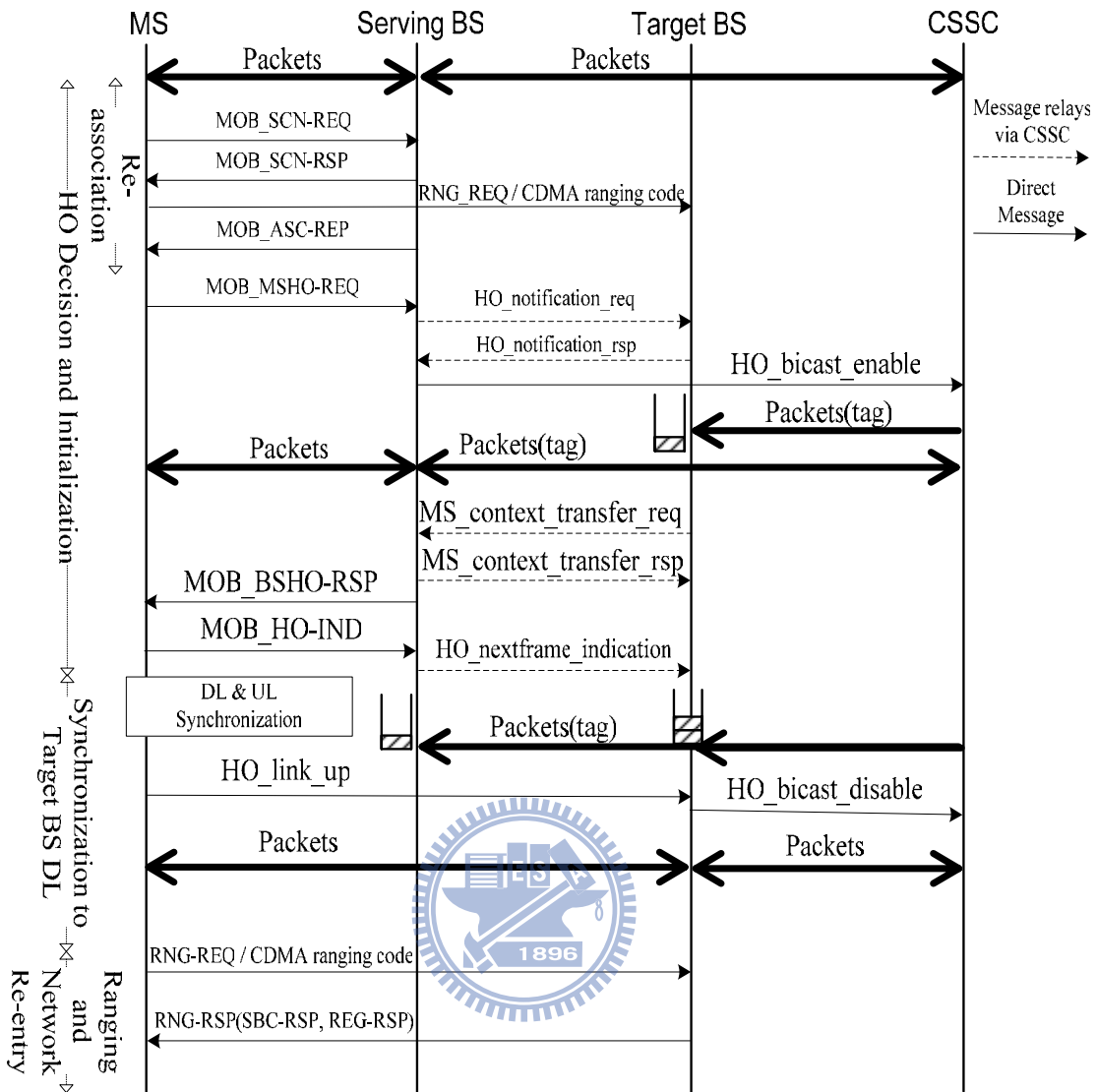
Fig. 3.5: Intra-CSSC HO MSC.

Fig. 3.5 shows the MSC of the proposed intra-CSSC NFHO scheme. The bold lines show packet flows and the others are management messages. The management messages with dashed lines exchanged between BSs are relayed via a CSSC. The management messages with solid lines are direct messages from source to destination. The management message terms with all capital letters are the MAC management messages defined in the IEEE 802.16e and the other management messages terms with leading capital letters and followed by low case letters are added messages for the NFHO scheme. The proposed intra-CSSC NFHO scheme that shortens service disruption time is detailed as follows:

1) After the HO target is selected in the HO Decision and Initialization stage, the MS starts a re-association to renew UL parameters for the target BS if the MS considers the current UL parameters of the target BS to be out-of-date. The renewed UL parameters will be used for UL synchronization in the Synchronization to Target BS DL stage.

2) When an MS issues MOB_MSHO-REQ to the serving BS, the serving BS should negotiate the QoS requirement of the MS with the target BS via the added backbone messages: HO_notification_req and HO_notification_rsp.

3) The serving BS issues an HO_bicast_enable message to enable bicasting DL packets to the target BS. After that, each DL packet bicast to both the serving and target BSs is tagged with a sequence number. In Fig. 3.5, we denote a tagged packet flow as Packets(tag).

4) Because the HO process optimization options are enabled to omit authorization, the serving and target BSs must use MS_context_transfer_req and MS_context_transfer_rsp to transfer the context of the MS. After that, the serving BS sends MOB_BSHO-RSP to the MS.

5) The MS sends MOB_HO-IND to inform the serving BS that the HO is started. Then, the MS enters the Synchronization to Target BS DL stage and starts synchronizing to the target BS. Meanwhile, the serving BS sends HO_nextframe_indication to notify the target BS of the tagged sequence number of the next expected DL packet. After synchronizing to the DL of the target BS, the MS also synchronizes to the UL by the acquired UL parameters described in section 3.1.1. As mentioned above, there is no need to update transport CIDs for the active connections of the MS during intra-CSSC HO. Therefore, the target BS can start to allocate DL_MAP_IE and UL_MAP_IE for DL and UL data packets after receiving HO_link_up. The MS sends HO_link_up to inform the target BS of UL synchronization. Note that the HO_link_up could be a bandwidth request packet instead. After that, the target BS issues HO_bicast_disable to disable bicasting and let the DL data path switch to the target BS only.

6) The HO ranging, which exchanges RNG-REQ and RNG-RSP, is started after normal data

packet transmission. Since the HO optimization options are enabled, the unsolicited SBC-RSP (Basic Capabilities Negotiation) and REG-RSP (Registration) are appended to the RNG-RSP.

Fig. 3.6 shows the MSC for the proposed inter-CSSC NFHO scheme. The MSC is similar to that of the intra-CSSC HO except that the target CSSC updates transport CIDs for the active connections of the MS, and these updated transport CIDs are sent back to the MS through MOB_BSHO-RSP. The message followed by "(CIDs)" denotes that these updated transport CIDs are attached. The following details the inter-CSSC HO MSC.

1) The MS performs association level 2 to the selected target BS and then obtains UL parameters from MOB_ASC-REP.

2) The MS starts an HO by issuing MOB_MSHO-REQ to the serving BS. The serving BS uses HO_notification_req to negotiate MS's QoS requirements with the target BS. Since this HO is an inter-CSSC HO, the target CSSC needs to update transport CIDs for the active connections of the MS. The target BS requests a connection setup to the target CSSC by sending HO_connection_setup_req. Then the target CSSC assigns transport CIDs and initializes a classifier which will classify upcoming bicasting packets by the assigned transport CIDs. The target CSSC sends HO_connection_setup_complete with assigned transport CIDs to the target BS. Finally, the assigned transport CIDs are delivered to the serving BS through HO_notification_rsp.

3) The HO_bicast_enable is issued by the serving BS to enable bicasting DL data packets to the target CSSC. After that, each DL packet tagged with a sequence number is bicast to both the serving and target BSs. The target CSSC and target BS will use the assigned transport CIDs to transmit packets.

4) MS_context_transfer_req and MS_context_transfer_rsp are used to transfer the context of the

MS from the serving BS to the target BS. The serving BS sends an MOB_BSHO-RSP message with the assigned transport CIDs appended to respond to the received MOB_MSHO-REQ.

5) After sending MOB_HO-IND, the MS enters the Synchronization to the target BS DL stage. After synchronizing to the DL, the MS also immediately synchronizes to the UL by the acquired UL parameters described in section 3.1.1. The serving BS sends the target BS HO_nextframe_indication to notify the next expected sequence number of the tagged DL packet. Since the connection setup between the target BS and the target CSSC have been done and the bicast DL packets in the target BS have been constructed with assigned transport CIDs, the target BS can go ahead to schedule for UL/DL data transmission without waiting for the completion of the HO ranging. The HO_link_up issued by the MS is used to indicate that the MS has synchronized to the UL of the target BS; therefore, the HO_link_up could be a bandwidth request packet instead of a specific management message. After that, the target BS sends HO_bicast_disable to switch the DL data path to the target BS only.

6) The HO ranging is started after normal data packet transmission. Since the target BS enables the HO optimization options, the unsolicited SBC-RSP and REG-RSP are appended to the RNG-RSP.
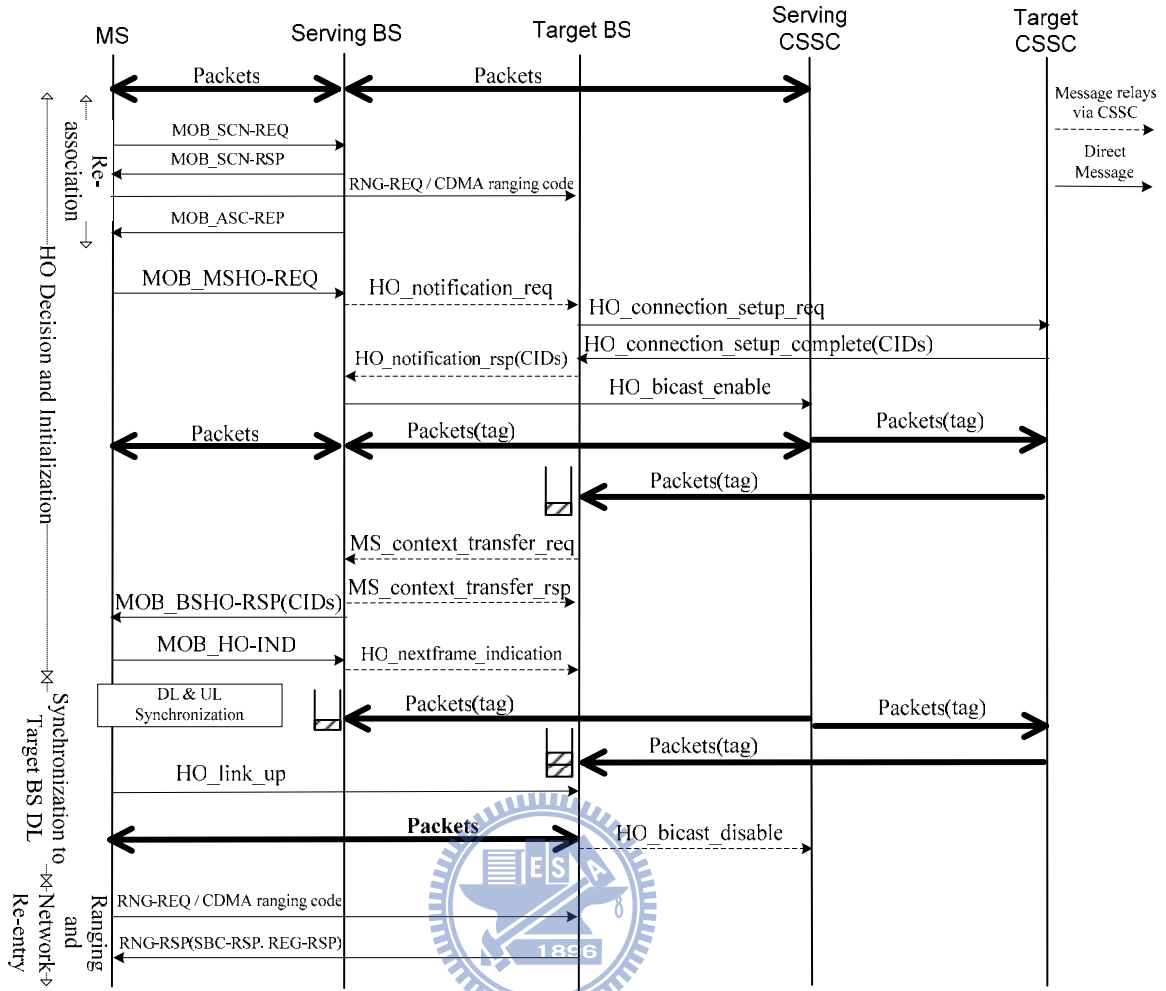
Fig. 3.6: Inter-CSSC HO MSC.

3.2 Analytic Model

Since the proposed NFHO scheme bicasts DL packets to the target BS in advance in addition to the serving BS, the expected number of buffered packets in the target BS is a performance metric. The exhaustion of the packet buffer pool may result in the packet loss of subsequent incoming DL packets, and the packet loss probability is another performance metric to evaluate the QoS for the MS. Therefore, including the packet loss probability to the policy of admission control is necessary to guarantee QoS to the ongoing HO MSs.

In the following, we focus on the inter-CSSC HO and analyze the expected number of buffered packets in section 3.2.1. In section 3.2.2, with a limited packet buffers constraint, we

36

analyze the number of concurrent HO MSs and the packet loss probability from a system viewpoint. In section 3.2.3, we evaluate existing HO schemes and analyze the service disruption time and the expected number of buffered packets during an HO. By applying the expected number of buffered packets obtained in section 3.2.3 to the derivations in section 3.2.2, we can obtain the packet loss probability for each existing HO scheme.
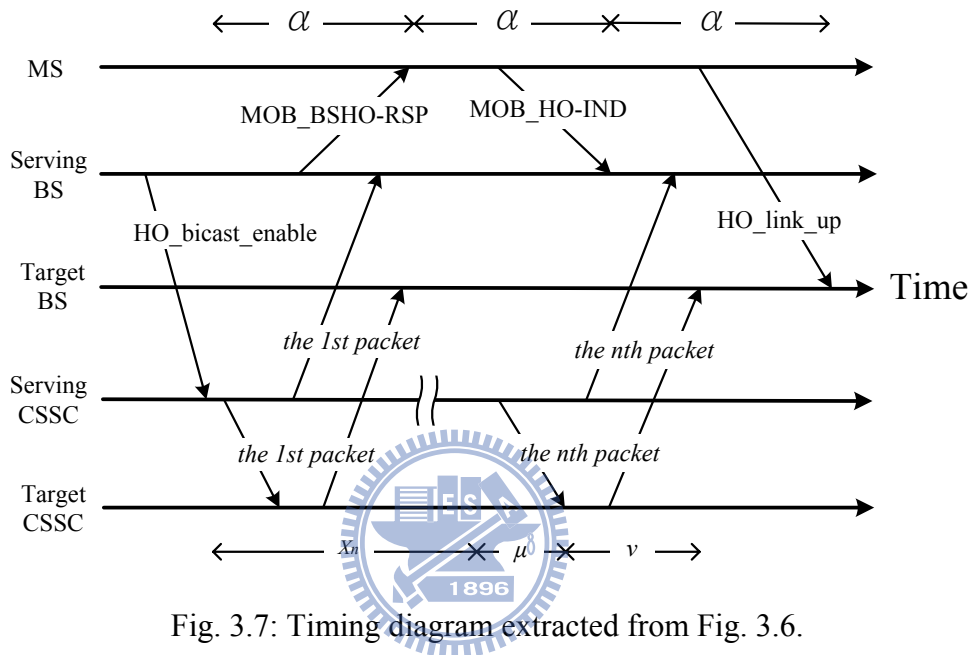
Fig. 3.7: Timing diagram extracted from Fig. 3.6.

3.2.1 Expected Number of Buffered Packets

Fig. 3.7 shows the timing diagram extracted from Fig. 3.6. After the HO_bicast_enable arrives at the serving CSSC, the serving CSSC starts to bicast subsequent DL packets to the serving BS and the target BS. The packets bicast to the target BS are buffered in the buffer pool until the MS synchronizes to the DL of the target BS and informs the target BS of UL synchronization by issuing an HO_link_up. After the target BS receives the HO_link_up, the buffered packets start to be consumed by sending them to the MS. Therefore, in the target BS, the number of packets buffered for the MS will reach a maximum at the moment that the HO_link_up arrives at the target BS. Assume that the arrival of packets to the serving CSSC is a Poisson arrival process

with arrival rate λ [16][18]. Thus, the interarrival times are exponentially distributed. Assume an HO_bicast_enable arrives at the serving CSSC at time t_0, and t_n is the time that the nth packet arrives at the serving CSSC. Let $X_n = t_n - t_0$ denote the nth bicast packet arriving at the serving CSSC in the period [0, t]. Thus, X_n has an Erlang distribution with density function [18][20]

$$f_{X_n}(t) = \frac{(\lambda t)^{n-1}}{(n-1)!} \lambda e^{-\lambda t}$$

(1)

And the Laplace transform for X_n is

$$f_{X_n}^*(s) = \left(\frac{\lambda}{s + \lambda} \right)^n$$

(2)

Without loss of generality, we assume the processing delays of HO_BSHO-RSP, MOB_HO-IND, and HO_link_up have the same distribution with mixed-Erlang density function [18][19][21]

$$f_\alpha(t) = \sum_{i=1}^{I} \alpha_i \frac{(\sigma_i t)^{p_i - 1}}{(p_i - 1)!} \sigma_i e^{-\sigma_i t}$$

(3)

where

$$\sum_{i=1}^{I} \alpha_i = 1$$

and α is a random variable to represent the processing delay. The Laplace transform for α is expressed as

$$f_\alpha^*(s) = \sum_{i=1}^{I} \alpha_i \left(\frac{\sigma_i}{s + \sigma_i} \right)^{p_i}$$

(4)

We select the mixed Erlang distribution because it has been proven that it can well approximate to many other distributions [17][18][21].

Let μ be a random variable to denote the transmission delay from the serving CSSC to the target CSSC, and ν is a random variable to denote the transmission delay from the target CSSC to the target BS. Thus, the transmission delay from the serving CSSC to the target BS is $\mu + \nu$. Assume

that both μ and ν also have the mixed Erlang distributions with the following density functions [18][19][21]

$$f_\mu(t) = \sum_{j=1}^{J} \mu_j \frac{(\rho_j t)^{q_j-1}}{(q_j-1)!} \rho_j e^{-\rho_j t}$$

(5)

$$f_\nu(t) = \sum_{k=1}^{K} \nu_k \frac{(\delta_k t)^{r_k-1}}{(r_k-1)!} \delta_k e^{-\delta_k t}$$

(6)

where

$$\sum_{j=1}^{J} \mu_j = 1 \quad \text{and} \quad \sum_{k=1}^{K} \nu_k = 1$$

The corresponding Laplace transforms are expressed as follows

$$f_\mu^*(s) = \sum_{j=1}^{J} \mu_j \left(\frac{\rho_j}{s+\rho_j} \right)^{q_j}$$

(7)

$$f_\nu^*(s) = \sum_{k=1}^{K} \nu_k \left(\frac{\delta_k}{s+\delta_k} \right)^{r_k}$$

(8)

Let Φ_n represent the nth packet that arrives at the target BS. From Fig. 3.7, we have

$$\Phi_n = \begin{cases} 1 & X_n + \mu + \nu < 3\alpha \\ 0 & otherwise \end{cases}$$

(9)

Therefore, the expected number of buffered packets, denoted as Q_{max}, is expressed as [18]

$$Q_{max} = \sum_{n=1}^{\infty} E(\Phi_n)$$

(10)

$$= \sum_{n=1}^{\infty} \Pr(X_n + \mu + \nu < 3\alpha)$$

(11)

Let $T_n = X_n + \mu + \nu$, then (10) can be rewritten as

$$Q_{max} = \sum_{n=1}^{\infty} \Pr(T_n < 3\alpha)$$

(12)

where $\Pr(T_n < 3\alpha)$ is calculated as

$$= \sum_{n=1}^{\infty} \left\{ \int_{T=0}^{\infty} f_{T_n}(T) \left[\int_{t=T}^{\infty} f_{3\alpha}(t)dt \right] dT \right\}$$

$$= \sum_{n=1}^{\infty} \left\{ \int_{T=0}^{\infty} f_{T_n}(T) \left[\sum_{i=1}^{I} \frac{\alpha_i \sigma_i^{P_i}}{3^{P_i}(P_i-1)!} \left(\int_{t=T}^{\infty} t^{P_i-1} e^{-\frac{\sigma_i}{3}t} dt \right) \right] dT \right\}$$

$$= \sum_{n=1}^{\infty} \left\{ \int_{T=0}^{\infty} f_{T_n}(T) \left[\sum_{i=1}^{I} \alpha_i \left(\sum_{h=0}^{P_i-1} \frac{(\sigma_i T)^h}{3^h h!} e^{-\frac{\sigma_i}{3}T} \right) \right] dT \right\}$$

$$= \sum_{n=1}^{\infty} \sum_{i=1}^{I} \alpha_i \sum_{h=0}^{P_i-1} \frac{\sigma_i^h}{3^h h!} \left(\int_{T=0}^{\infty} f_{T_n}(T) T^h e^{-\frac{\sigma_i}{3}T} dT \right)$$

$$= \sum_{n=1}^{\infty} \sum_{i=1}^{I} \alpha_i \sum_{h=0}^{P_i-1} \frac{\sigma_i^h}{3^h h!} \left((-1)^h \frac{d^h}{ds^h} f_{T_n}^*(s) \bigg|_{s=\frac{\sigma_i}{3}} \right)$$

(13)

Since $T_n = X_n + \mu + v$ and $f_{T_n}(t)$ denotes the density function of T_n, by applying the convolution property, its Laplace transform, $f_{T_n}^*(s)$, is as follows:

$$f_{T_n}^* = f_{X_n}^* f_\mu^* f_v^*$$

$$= \left(\frac{\lambda}{s+\lambda} \right)^n \left[\sum_{j=1}^{J} \mu_j \left(\frac{\rho_j}{s+\rho_j} \right)^{q_j} \right] \left[\sum_{k=1}^{k} v_k \left(\frac{\delta_k}{s+\delta_k} \right)^{r_k} \right]$$
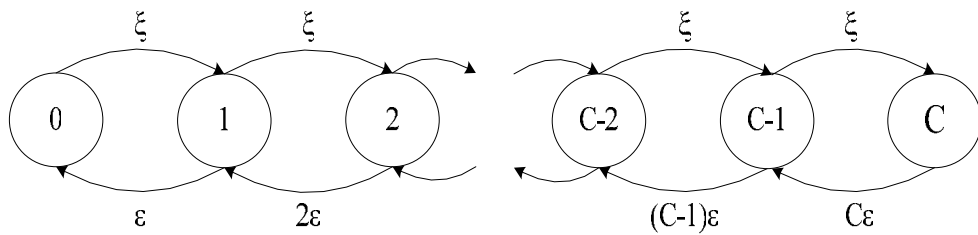
(14)

Fig. 3.8: State transition diagram for HO processing.

3.2.2 Packet Loss Probability during Handover

Since the target BS only has limited packet buffers to queue bicast packets during HO, bicast packets arrived at the target BS are dropped if there is no available packet buffer. Suppose the BS could provide a common HO packet buffer pool to hold bicast packets for all incoming HO

MSs. After the HO_link_up is received, the BS allocates the MS a dedicated connection buffer pool. Then, the buffered packets for the MS are moved from the HO packet buffer pool to the MS's dedicated connection buffer pool, and the packet buffers are released to the HO packet buffer pool immediately.

Consider a BS that can handle at most C MSs that handover into the BS concurrently. Assume that the arrival of an HO request is a Poisson process with arrival rate ξ. The HO processing time is exponentially distributed with mean $1/\varepsilon$. We model the HO processing as M/M/m/m queuing model. Fig. 3.8 shows the state transition of the Markov process for HO processing. The arrival rate of state k in this model is

$$\xi_k = \begin{cases} \xi & k < C \\ 0 & k \geq C \end{cases}$$

(15)

The departure rate in state k is given by

$$\varepsilon_k = k\varepsilon$$

(16)

Let the probability in state k be π_k; therefore, we have

$$\sum_{k=0}^{C} \pi_k = 1$$

(17)

From [20], we have

$$\pi_k = \begin{cases} \pi_0 \prod_{i=0}^{k-1} \frac{\xi}{(i+1)\varepsilon} & k \leq C \\ 0 & k > C \end{cases}$$

(18)

Substitute π_k into (17), we get

$$\pi_0 = \left[\sum_{k=0}^{C} \left(\frac{\xi}{\varepsilon} \right)^k \frac{1}{k!} \right]^{-1}$$

(19)

To analyze the usage of the HO packet buffer pool, we model it as an M/M/m/m queuing model. Assume that the HO packet buffer pool can provide at most m packet buffers. Fig. 3.9 shows the state transition of the Markov process for the utilization of HO packet buffers. The

buffer requests to the HO packet buffer pool is a Poisson arrival process with rate ϖ. The buffer request rate can be obtained from the expected number of on-going HO MSs and the packet arrival rate of each on-going HO MS. Therefore, ϖ can be expressed as

$$\varpi = \lambda \sum_{k=1}^{C} k \pi_k \tag{20}$$
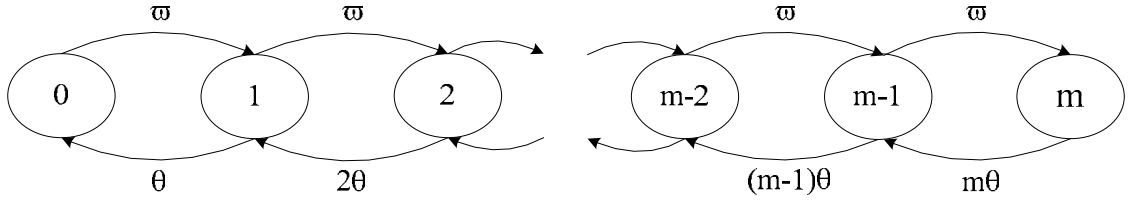
Fig. 3.9: State transition diagram for packet buffer utilization.

Let θ denote the rate of the HO packet buffers that are released to the HO packet buffer pool. And, an HO packet buffer holding time, Θ, can be expressed as $\Theta = 1/\theta$. Let Th_n denote the duration of the nth bicast packet that is buffered at the target BS. Thus, the expected time of a bicast packet held at the target BS can be obtained

$$\Theta = Q_{max}^{-1} \sum_{n=1}^{\infty} E(Th_n) \tag{21}$$

where $E(Th_n)$ is calculated as follows:

$$E(Th_n) = \int_{T=0}^{\infty} \int_{t=T}^{\infty} f_{T_n}(T) f_{3\alpha}(t)(t-T)\,dt\,dT$$

$$= \int_{T=0}^{\infty} \int_{t=T}^{\infty} f_{T_n}(T) f_{3\alpha}(t)\,t\,dt\,dT \quad -$$

$$\int_{T=0}^{\infty} \int_{t=T}^{\infty} f_{T_n}(T) f_{3\alpha}(t)\,T\,dt\,dT$$

$$= \sum_{i=1}^{I} \alpha_i \left[\sum_{h=0}^{P_i} \frac{p_i \sigma_i^{h-1}}{3^{h-1} h!} \left(\int_{T=0}^{\infty} f_{T_n}(T) T^h e^{-\frac{\sigma_i T}{3}} dT \right) \right] -$$

$$\sum_{i=1}^{I} \alpha_i \left[\sum_{h=0}^{P_i-1} \frac{\sigma_i^h}{3^h h!} \left(\int_{T=0}^{\infty} f_{T_n}(T) T^{h+1} e^{-\frac{\sigma_i T}{3}} dT \right) \right]$$

$$= \sum_{i=1}^{I} \alpha_i \left\{ \left[\sum_{h=0}^{P_i} \frac{p_i \sigma_i^{h-1}}{3^{h-1} h!} \left((-1)^h \frac{d^h}{ds^h} f_{T_n}^*(s) \Big|_{s=\frac{\sigma_i}{3}} \right) \right] - \left[\sum_{h=0}^{P_i-1} \frac{\sigma_i^h}{3^h h!} \left((-1)^{h+1} \frac{d^{h+1}}{ds^{h+1}} f_{T_n}^*(s) \Big|_{s=\frac{\sigma_i}{3}} \right) \right] \right\}$$

(22)

In this model, the packet buffer request rate in state k is

$$\varpi_k = \begin{cases} \varpi & k < m \\ 0 & k \geq m \end{cases}$$

(23)

The packet buffer release rate in state k is

$$\theta_k = k \theta$$

(24)

Assuming the probability in state k denoted as ψ_k, we have

$$\sum_{k=0}^{m} \psi_k = 1$$

(25)

Thus, from [20], the probability in state k is

$$\psi_k = \psi_0 \prod_{i=0}^{k-1} \frac{\varpi}{(i+1)\theta} \qquad k \leq m$$

(26)

Substituting ψ_k into Eq. (25), we have

$$\psi_0 = \left[\sum_{k=0}^{m} \left(\frac{\varpi}{\theta} \right)^k \frac{1}{k!} \right]^{-1}$$

(27)

3.2.3 Service Disruption Time during the HO Execution Procedure

The service disruption time is defined as the duration that the MS and BS stop data transmission during the HO Execution procedure. In this section, we evaluate existing HO schemes, including the proposed NFHO, and analyze the service disruption time for the HO Execution procedure of each scheme. We assume that the HO process optimization options are enabled to omit the basic

capabilities negotiation and authorization in the HO Execution procedure. First, the following parameters are defined:

T_{Sync} Mean time of the DL synchronization

T_{Rng} Mean time of the HO ranging

T_{Reg} Mean time of the registration

In Table 3.1, the service disruption time of some classical HO schemes and the proposed NFHO scheme are compared. Since the schemes in [14], [15], and the proposed NFHO can immediately restart the DL transmission after the Synchronization to Target BS Downlink stage, these schemes have the same DL service disruption time and shorter DL disruption time than the IEEE 802.16e hard HO scheme. The scheme in [15] can temporarily use transport CIDs until these CIDs are updated in the registration. Thus, it can restart the UL transmission immediately after the HO ranging. In [14], it only improves on DL transmission, so it has the same UL service disruption time with the IEEE 802.16e hard HO scheme. By resolving transport CIDs assignment and UL synchronization issues, the proposed NFHO can also restart the UL transmission immediately after the Synchronization to Target BS Downlink stage.

TABLE 3.1: SERVICE DISRUPTION TIME OF THE EXISTING HO SCHEMES

SCHEME	DL	UL
802.16e [2]	$T_{Sync} + T_{Rng} + T_{Reg}$	$T_{Sync} + T_{Rng} + T_{Reg}$
Choi et al. [14]	T_{Sync}	$T_{Sync} + T_{Rng} + T_{Reg}$
Jiao et al. [15]	T_{Sync}	$T_{Sync} + T_{Rng}$
Proposed NFHO	T_{Sync}	T_{Sync}

We assume that both the DL and UL have the same traffic model and define Y_n as the nth packet arrived at the target BS in the DL part or generating from the MS in the UL part during the service disruption time. Assume Y_n has an Erlang distribution with the following density function [18][20]:

$$f_{Y_n}(t) = \frac{(\lambda t)^{n-1}}{(n-1)!} \lambda e^{-\lambda t}$$

(28)

And, the Laplace transform for the density function of Y_n is

$$f_{Y_n}^*(s) = \left(\frac{\lambda}{s+\lambda} \right)^n$$

(29)

Let *R1, R2,* and *R3* be random variables to represent the processing times of DL synchronization, HO ranging, and registration, respectively. Assume R1, R2, and R3 also have mixed Erlang distributions with the following density functions [18][19][21]:

$$f_{R1}(t) = \sum_{i=1}^{I} a_i \frac{(\beta_i t)^{p_i-1}}{(p_i-1)!} \beta_i e^{-\beta_i t}$$

(30)

$$f_{R2}(t) = \sum_{j=1}^{J} b_j \frac{(\phi_j t)^{q_j-1}}{(q_j-1)!} \phi_j e^{-\phi_j t}$$

(31)

$$f_{R3}(t) = \sum_{k=1}^{K} c_k \frac{(\varphi_k t)^{r_k-1}}{(r_k-1)!} \varphi_k e^{-\varphi_k t}$$
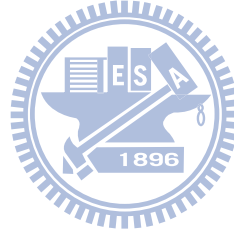
(32)

where

$$\sum_{i=1}^{I} a_i = 1, \quad \sum_{j=1}^{J} b_j = 1, \text{ and } \sum_{k=1}^{K} c_k = 1$$

The corresponding Laplace transforms are shown as follows:

$$f_{R1}^*(s) = \sum_{i=1}^{I} a_i \left(\frac{\beta_i}{s+\beta_i} \right)^{p_i}$$

(33)

$$f_{R2}^*(s) = \sum_{j=1}^{J} b_j \left(\frac{\phi_j}{s+\phi_j} \right)^{q_j}$$

(34)

45

$$f_{R3}^*(s) = \sum_{k=1}^{K} c_k \left(\frac{\varphi_k}{s + \varphi_k} \right)^{r_k} \tag{35}$$

Let Γ_n denote the nth packet that is buffered during the service disruption time. In the DL part, Γ_n denotes the nth packet that is buffered at the BS, and in the UL part, Γ_n denotes the nth packet that is buffered at the MS during the service disruption time. Then, we have

$$\Gamma_n = \begin{cases} 1 & Y_n \le R1 + R2 + R3 \\ 0 & otherwise \end{cases} \tag{36}$$

Let Q_{sdt} denote the number of buffered packets during the serving disruption time (sdt). Therefore, Q_{sdt} can be expressed as

$$Q_{sdt} = \sum_{n=1}^{\infty} E(\Gamma_n) \tag{37}$$

$$= \sum_{n=1}^{\infty} \Pr(Y_n \le R1 + R2 + R3) \tag{38}$$

Let $T_e = R1 + R2 + R3$, then (38) can be rewritten as

$$= \sum_{n=1}^{\infty} \Pr(Y_n \le T_e)$$

$$= \sum_{n=1}^{\infty} \int_{T=0}^{\infty} f_{T_e}(T) \left[\int_{t=0}^{T} \frac{\lambda^n t^{n-1}}{(n-1)!} e^{-\lambda t} dt \right] dT$$

$$= \sum_{n=1}^{\infty} \int_{T=0}^{\infty} f_{T_e}(T) \left[1 - \sum_{k=0}^{n-1} (\frac{\lambda^k}{k!}) T^k e^{-\lambda T} \right] dT$$

$$= \sum_{n=1}^{\infty} \left[\int_{T=0}^{\infty} f_{T_e}(T) dT - \sum_{k=0}^{n-1} (\frac{\lambda^k}{k!}) \int_{T=0}^{\infty} f_{T_e}(T) T^k e^{-\lambda T} dT \right]$$

$$= \sum_{n=1}^{\infty} \left[f_{T_e}^*(s) |_{s=0} + \sum_{k=0}^{n-1} (-1)^{k+1} (\frac{\lambda^k}{k!}) \frac{d^k}{ds^k} f_{T_e}^*(s) |_{s=\lambda} \right] \tag{39}$$

Since $T_e = R1+R2+R3$ and $f_{T_e}(t)$ denote the density function of T_e, by applying the convolution property, its Laplace transform, $f_{T_e}^*(s)$, is as follows:

$$f_{T_e}^* = f_{R1}^* f_{R2}^* f_{R3}^*$$

$$= \left[\sum_{i=1}^{I} a_i \left(\frac{\beta_i}{s+\beta_i} \right)^{p_i} \right] \left[\sum_{j=1}^{J} b_j \left(\frac{\phi_j}{s+\phi_j} \right)^{q_j} \right] \left[\sum_{k=1}^{K} c_k \left(\frac{\varphi_k}{s+\varphi_k} \right)^{r_k} \right]$$

(40)

Let Tb_n denote the duration of the nth packet that is buffered at the target BS (DL part) or the MS (UL part). Thus, the mean time of a packet buffered in the target BS (DL part) or in the MS (UL part) can be expressed as

$$\Theta = Q_{sdt}^{-1} \sum_{n=1}^{\infty} E(Tb_n)$$

(41)

$$= Q_{sdt}^{-1} \sum_{n=1}^{\infty} \int_{T=0}^{\infty} f_{T_e}(T) \int_{t=0}^{T} f_{Y_n}(t)(T-t)\,dt\,dT$$

$$= Q_{sdt}^{-1} \sum_{n=1}^{\infty} \left[\begin{array}{l} \int_{T=0}^{\infty} f_{T_e}(T)T \int_{t=0}^{T} f_{Y_n}(t)\,dt\,dT - \\ \int_{T=0}^{\infty} f_{T_e}(T) \int_{t=0}^{T} f_{Y_n}(t)t\,dt\,dT \end{array} \right]$$

$$= Q_{sdt}^{-1} \sum_{n=1}^{\infty} \left\{ \begin{array}{l} \left[\int_{T=0}^{\infty} f_{T_e}(T)T\,dT - \sum_{k=0}^{n-1} \frac{\lambda^k}{k!} \int_{T=0}^{\infty} T^{k+1} e^{-\lambda T}\,dT \right] - \\ \left(\frac{n}{\lambda} \right) \left[\int_{T=0}^{\infty} f_{T_e}(T)\,dT - \sum_{k=0}^{n} \frac{\lambda^k}{k!} \int_{T=0}^{\infty} f_{T_e}(T) T^k e^{-\lambda T}\,dT \right] \end{array} \right\}$$

$$= Q_{sdt}^{-1} \sum_{n=1}^{\infty} \left\{ \begin{array}{l} (-1)\left(\frac{d}{ds} f_{T_e}^*(s)\big|_{s=0} + \frac{n}{\lambda} f_{T_e}^*(s)\big|_{s=0} \right) + \frac{n}{\lambda} f_{T_e}^*(s)\big|_{s=\lambda} + \\ \sum_{k=0}^{n-1} (-1)^k \frac{\lambda^k}{k!} \left[\frac{k+1-n}{k+1} \right] \frac{d^{k+1}}{ds^{k+1}} f_{T_e}^*(s)\big|_{s=\lambda} \end{array} \right\}$$

(42)

47

TABLE 3.2: PARAMETER SETTINGS FOR PERFORMANCE EVALUATION.

VARIABLE	PARAMETERS
R1	$a_1 = a_2 = 0.5$ $\beta_1 = 200$, $\beta_2 = 66.67$ (packets/sec)
R2	$b_1 = b_2 = 0.5$ $\phi_1 = 100$, $\phi_2 = 66.67$ (packets/sec)
R3	$c_1 = c_2 = 0.5$ $\varphi_1 = 100$, $\varphi_2 = 40$ (packets/sec)
M	200 (packets)
ξ/ε	20

3.3 Performance Evaluation

Based on the analytic model derived in the last section, we first present analytic results of various IEEE 802.16e HO enhanced schemes, including the proposed NFHO scheme. A simulation model using NS-2 was also developed to validate the analytic model. The simulation model is based on the analytic model described in section 3.2.3. The same parameter settings shown in Table 3.2 [18] were used for simulation as well as for analysis. In the simulation, the packet interarrival time and the processing times for DL synchronization, HO ranging, and registration were generated by the random functions of their corresponding distributions. If a BS accepts an incoming HO MS, the service disruption time and the packet arrival time of each packet during the service disruption time can be computed. Thus, we can obtain the expected number of buffered packets. Furthermore, the packet loss probability can be obtained by monitoring the usage of the HO packet buffer pool. In section 3.3.1, the performance evaluation results, including analytic and simulation results, are compared among the existing HO schemes

and the proposed NFHO scheme. In addition, based on the analytic model of the proposed

inter-CSSC HO procedure, section 3.3.2 presents the expected number of buffered packets and

the packet loss probability of the proposed NFHO.
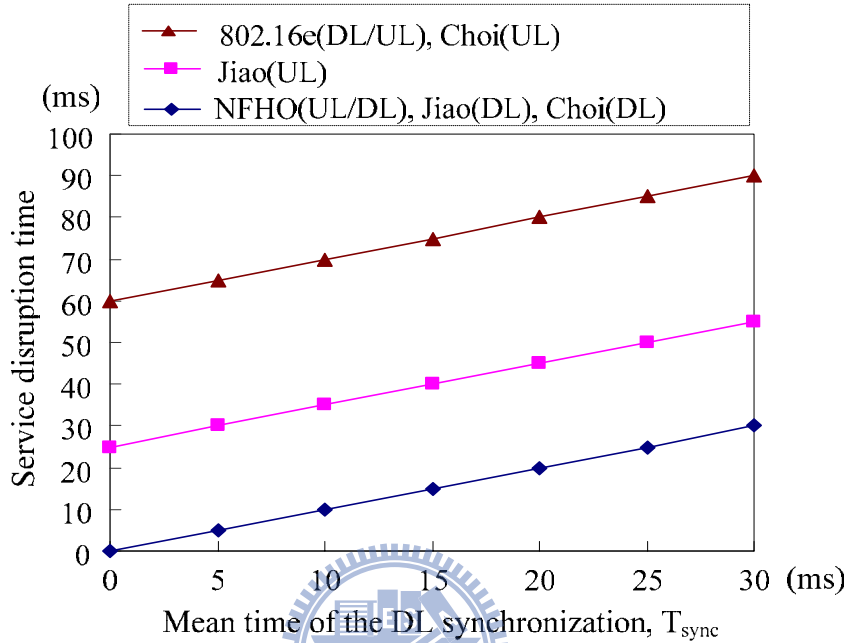
Fig. 3.10: HO service disruption time versus T_{Sync}

3.3.1 Performance Evaluation Results among the Existing HO Schemes

and the Proposed NFHO Scheme

To evaluate the proposed NFHO scheme with respect to the existing HO schemes, we first

compare the service disruption time. Based on Table 3.1, Fig. 3.10 shows the analytic results of

the service disruption time. The values of T_{Rng} and T_{Reg} were set to 25 *ms* and 35 *ms* [14],

respectively. We found that, in the DL part, the existing HO schemes and the proposed NFHO

scheme have the same service disruption time and all outperform the IEEE 802.16e HO scheme.

In the UL part, the NFHO scheme has shorter service disruption time than the other schemes. It

is because the NFHO scheme allows the UL data transmission to immediately restart after the

DL synchronization. Note that T_{Sync} is set to 20 *ms* [15]. From Fig. 3.10, it shows that the

proposed NFHO scheme reduces the DL service disruption time by 75% compared to the IEEE 802.16e HO scheme, and it also reduces the UL service disruption time by 55.6% compared to Jiao et al. [15] scheme and by 75% compared to both Choi et al. [14] scheme and the IEEE 802.16e HO scheme. As mentioned in section 3.1, only an add-on software component with a small cost is required to support the proposed NFHO scheme. Therefore, our NFHO scheme is cost-effective.
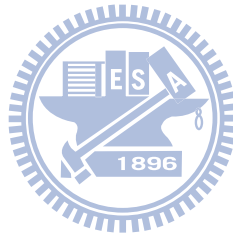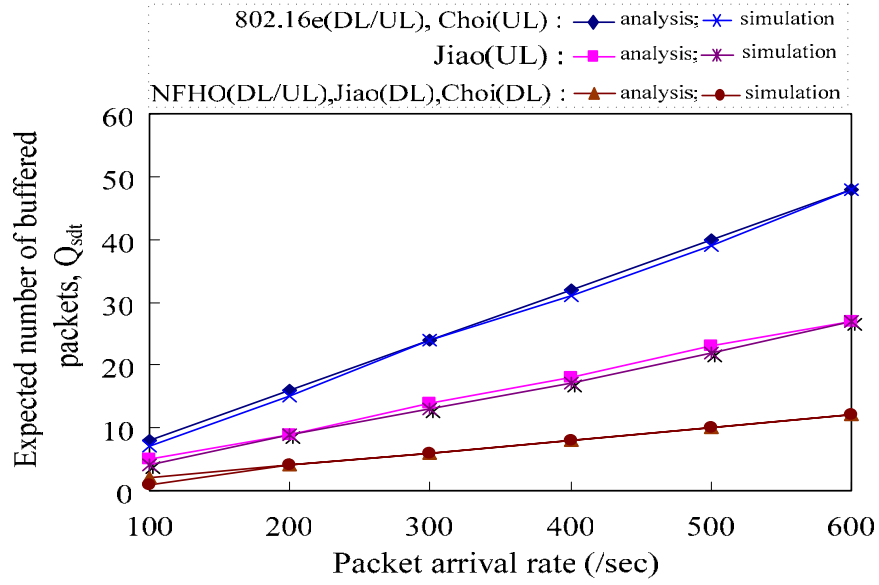
Fig. 3.11: Q_{sdt} versus packet arrival rate.
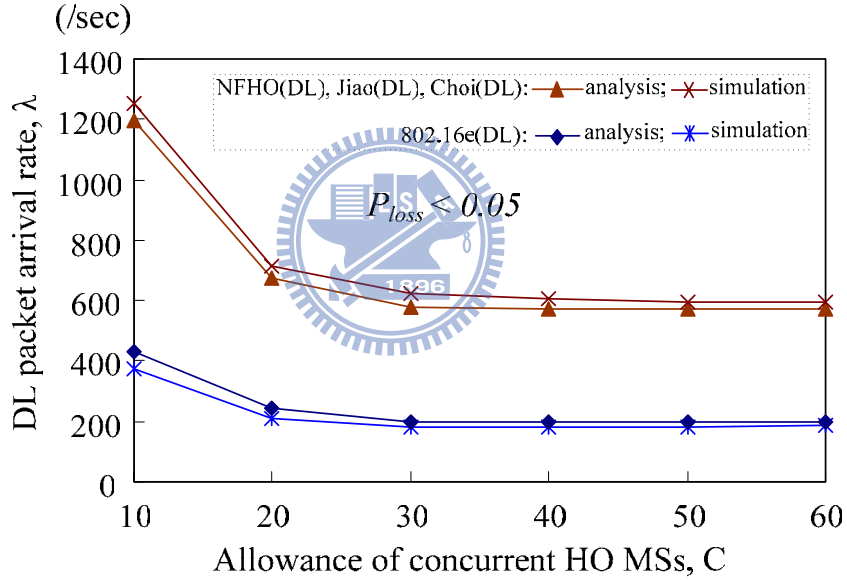
Fig. 3.12: Supported DL packet arrival rate versus the allowance of concurrent HO MSs under a given packet loss probability constraint ($P_{loss} < 0.05$).

In the following performance evaluation (Fig. 3.11 and Fig. 3.12), including analysis and simulation, the parameters listed in Table 3.2 [18] were used, unless there were individual parameter assignments in each evaluation. Note that even with other parameter settings, we can still obtain similar performance evaluation results. Assume that R1, R2, and R3 all have mixed Erlang-2 distributions. By Eq. (37), we investigate the expected number of buffered packets

(Q_{sdt}) among the proposed NFHO and the existing HO schemes. Fig. 3.11 shows the expected number of buffered packets during the HO Execution procedure. It can be seen that Q_{sdt} linearly increases with the increase of packet arrival rate, λ. This is because the packets are buffered in the BS (for DL packets) or the MS (for UL packets), and MS and BS stop transmitting during the service disruption time. The DL part of the proposed NFHO, Jiao et al. [15] and Choi et al. [14] schemes has the minimum Q_{sdt} because these schemes can restart DL transmission immediately after the DL is synchronized (R2 = R3 = 0). On the UL part, the Q_{sdt} of the proposed NFHO (R2 = R3 = 0) is the lowest, the Q_{sdt} of Jiao et al. (R3 = 0) is the next, and the Choi et al. and 802.16e HO schemes have larger Q_{sdt} than the others. In Fig. 3.11, the analytic and simulation results are very close, which confirms the validity of our analytic model.
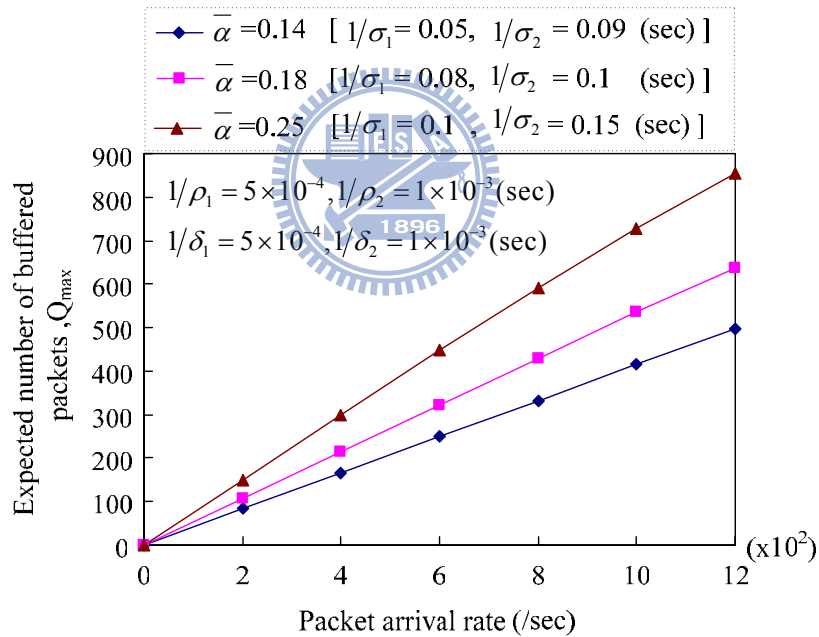
Fig. 3.13: Q_{max} versus packet arrival rate.

With a given packet loss probability constraint, by Eqs. (18), (26), (37), and (41), we analyze the relationship between the allowance of concurrent HO MSs (i.e., C) and the supported DL packet arrival rate (i.e., λ) per MS. We assume each MS has the same UL/DL packet rate. As shown in Fig. 3.12, by restricting the packet loss probability to be less than 0.05

during HO, in the DL part, the NFHO, Jiao et al., and Choi et al. schemes can support a higher

packet arrival rate than the IEEE 802.16e HO scheme. In Fig. 3.12, it also shows that λ becomes

stable even when C keeps increasing. It is because that a given ξ/ε ratio implies a limit (threshold)

on the number of concurrent HO MSs in a BS. λ gradually decreases until C exceeds by the

threshold. Again, in Fig. 3.12, the analytic and simulation results are very close, which confirms

the validity of our analytic model. Besides, in the UL part, the supported UL data rate depends

on the number of available packet buffers locally allocated in the MS. The UL performance

evaluation results among the proposed NFHO and the existing HO schemes has been shown in

Fig. 3.11. In the UL part of Fig. 3.11, with a given Q_{sdt}, we found that the NFHO scheme can

support a larger packet arrival rate than the other schemes. Note that a fixed Q_{sdt} is equivalent to

assign a P_{loss} because the available packet buffers are allocated in the MS.

$\lambda=170$ (cells/sec), $\xi/\varepsilon = 20$

$1/\sigma_1 = 0.08, 1/\sigma_2 = 0.1$(sec)

$1/\rho_1 = 5\times10^{-4}, 1/\rho_2 = 1\times10^{-3}$(sec)

$1/\delta_1 = 5\times10^{-4}, 1/\delta_2 = 1\times10^{-3}$(sec)
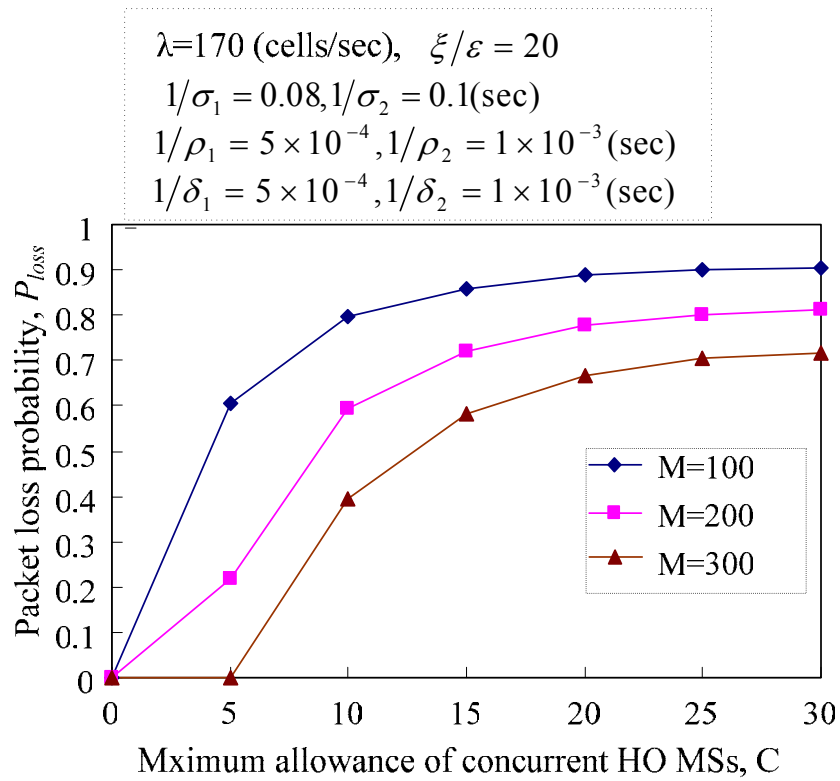
(a) Packet loss probability versus C
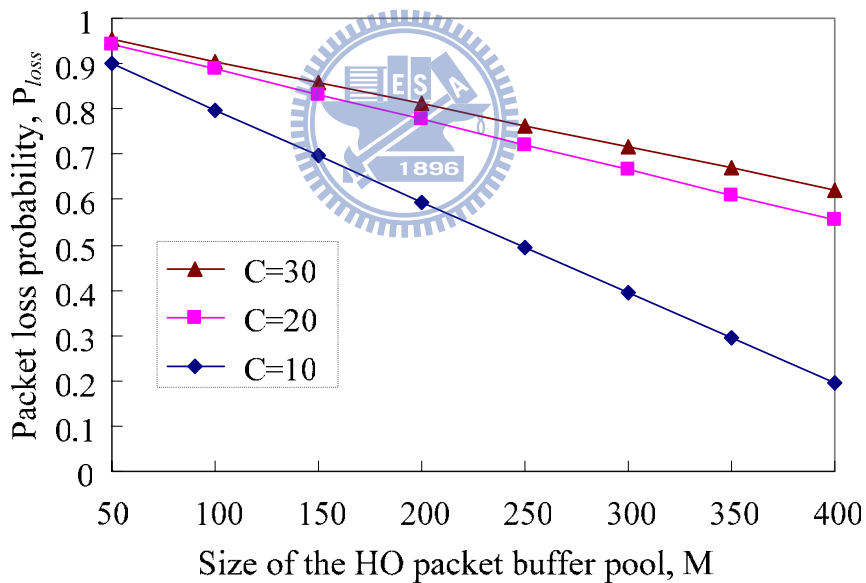
(b) Packet loss probability versus M

Fig. 3.14: Packet loss probabilities versus *C* and *M*.

3.3.2 Additional Performance Evaluation Results of the Proposed NFHO Scheme

With different transmission delays, α, we first investigate the relationship between the expected number of buffered packets in the target BS and the packet arrival rate. We assume random variables, μ, ν and α, have mixed Erlang-2 distributions [18][19][21]. The coefficients for μ, ν, and α were set to $\mu_1 = \mu_2 = 0.5$, $v_1 = v_2 = 0.5$, and $\alpha_1 = \alpha_2 = 0.5$, respectively [18]. Other parameter settings are shown in each figure. In addition, the mean time of HO message processing delay is computed as $\overline{\alpha} = 2(\alpha_1/\sigma_1 + \alpha_2/\sigma_2)$. By Eq. (10), Fig. 3.13 shows the relationship between the expected number of buffered packets in the target BS and the packet arrival rate under three different $\overline{\alpha}$. It was observed that the expected number of buffered packets (Q_{max}) is positively correlated to the packet arrival rate (λ) of the MS. An increase in λ leads to a larger Q_{max}, and a larger $\overline{\alpha}$ also results in a larger Q_{max}. Note that even with other parameter settings, we still can obtain similar results.

Since the size of the HO packet buffer pool is limited, the packet loss probability during HO is affected by the packet arrival rates of ongoing HO MSs and the available packet buffers in the pool. We consider three different sizes of the HO packet buffer pool, and the BS can only support a limited number of concurrent HO requests. By Eqs. (18), (21), and (26), we evaluate the relationship among C (the allowance of concurrent HO MSs), M (the size of the HO packet buffer pool), and P_{loss} (packet loss probability). Fig. 3.14(a) shows that the packet loss probability (P_{loss}) of an HO MS increases with the increase of the allowance of concurrent HO MSs (C). The BS that provides a larger size of HO packet buffer pool (M) has a lower packet loss probability during HO. Note that P_{loss} approximates zero when C and M are set to 5 and 300, respectively. This is because M is large enough to accommodate all arrival packets from C HO MSs. With the same traffic parameters, Fig. 3.14(b) also shows the relationship among P_{loss}, C,

and *M*. The parameter settings, listed on top of Fig. 3.14(a), will also be used in Fig. 3.15, Fig. 3.16, and Fig. 3.17, unless there are individual settings listed in each figure.
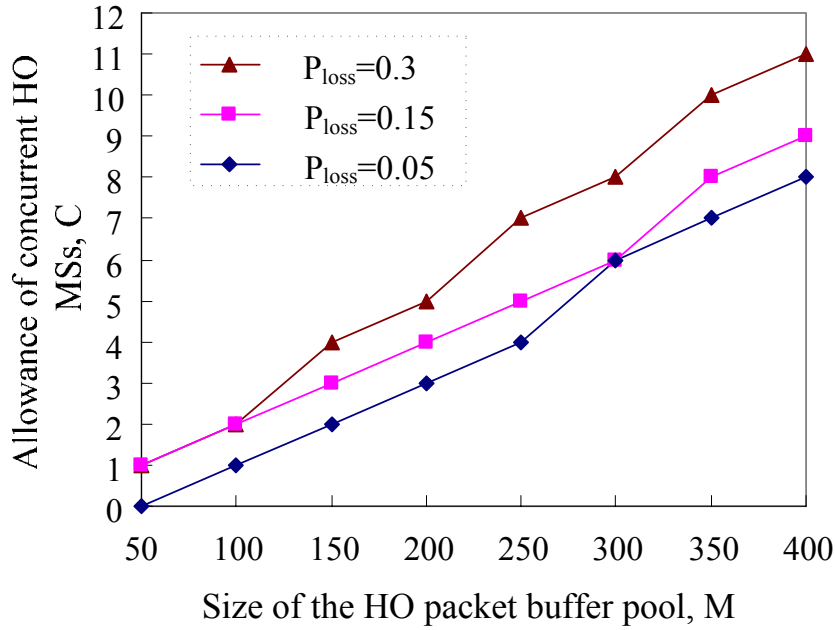
Fig. 3.15: The relationship between *M* (the size of the HO packet buffer pool) and *C* (the maximum allowance of concurrent HO MSs) under a given P_{loss} (packet loss probability) constraint.

Packet loss probability is an important QoS parameter for HO. According to the size of the HO packet buffer pool allocated in a BS, the BS can control the allowance of concurrent HO MSs to meet the packet loss probability requirement. With a given packet loss probability, by Eqs. (18), (21) and (26), we evaluate the relationship between *C* (the allowance of concurrent HO MSs) and *M* (the size of the HO packet buffer pool). Fig. 3.15 shows that when allocating a larger *M*, the BS can accept a higher *C* while still meeting the packet loss probability constraint. With a given P_{loss}, Fig. 3.16 also shows that the higher *C* that the BS allows, the lower λ (packet arrival rate) that the BS can support to each MS. Note that, without loss of generality, the ξ/ε ratio was set to 20, and *M* was set to 300. It can be observed that when we increase *C*, the supported λ of each MS decreases. The decreasing of λ is sharp until *C* is greater than 20. It is because the expected value of packet holding time grows until *C* exceeds the ξ/ε ratio. Similar

results are also shown in Fig. 3.17. Given three different ξ/ε ratios, it can be seen that when we increase C, P_{loss} grows sharply until C is greater than the corresponding ξ/ε ratio. Fig. 3.16 and Fig. 3.17 also show that the BS can guarantee the packet loss probability requirement for ongoing HO MSs by controlling the allowance of concurrent HO MSs (C) and the ξ/ε ratio. Therefore, to provide proper QoS (e.g., the packet loss probability, P_{loss}) to ongoing HO MSs, Eqs. (18), (21) and (26), which were the basis of Fig. 3.16 and Fig. 3.17, can assist to setup an appropriate admission control policy to grant or reject incoming HO requests.
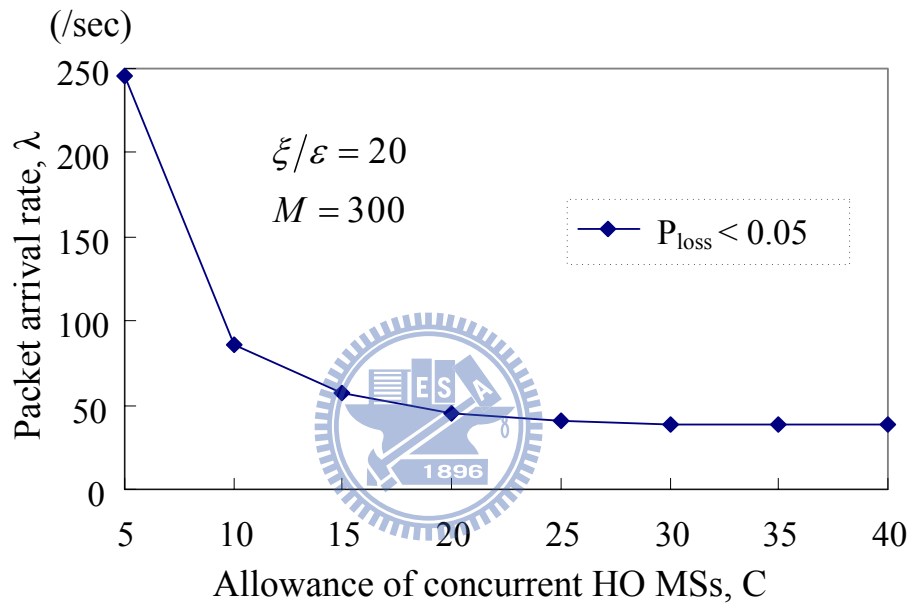

Fig. 3.16: Packet arrival rate (λ) of each MS versus the allowance of concurrent HO MSs (C)
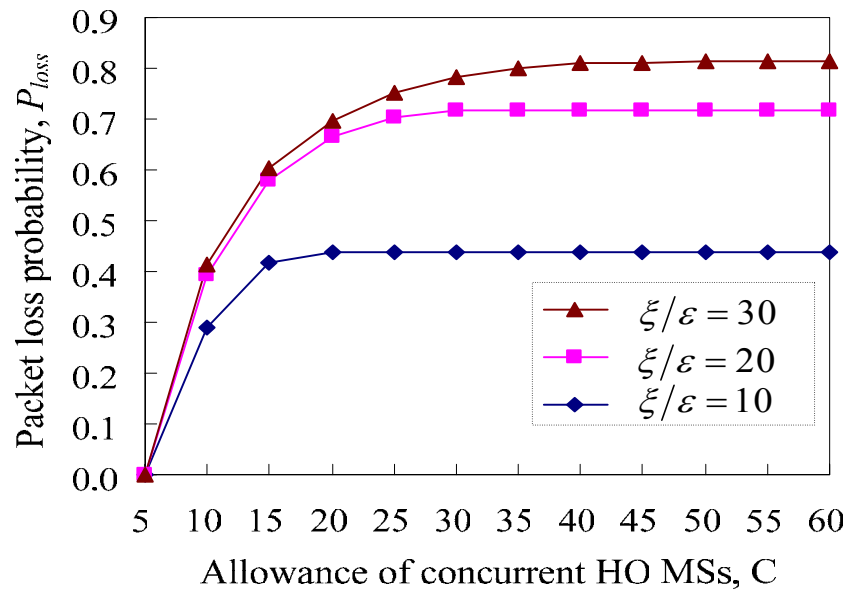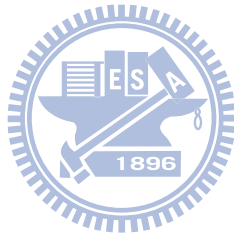
under a given packet loss probability (P_{loss}).

Fig. 3.17: P_{loss} versus C under a given ξ/ε.

Chapter 4

A Dynamic MBS Zone Framework for Cost-Effective Inter-MBS Zone Handover in WiMAX Networks

To synchronize MBS (multicast broadcast service) zone data transmission, the WiMAX standard defines a coordination mechanism to coordinate data transmission over the WiMAX network; however, the packet loss recovery procedures, which are parts of the coordination mechanism, enlarge the packet transmission latency and packet buffer pool requirement. In this Chapter, we propose an *in-frame control* (IFC) scheme to decrease the packet error rate and packet retransmission count, so as to reduce the packet transmission latency and packet buffer pool requirement. Furthermore, to support level-2 *frame-offset coordination*, we also propose a *dynamic MBS zone* (DMZ) framework that can provide data continuity between any two adjacent MBS zones. Based on the proposed DMZ framework, a seamless *dynamic inter-MBS zone handover* (called DMZ HO) scheme is proposed to resolve the data discontinuity (or packet loss) problem during inter-MBS zone HO. An analytic model has been developed to analyze the packet error rate and packet retransmission count for the proposed IFC scheme and the bandwidth overhead in terms of channel occupation time for the proposed DMZ HO. Performance evaluation results show that, compared to the original WiMAX scheme, defined in the WiMAX standard, the proposed IFC scheme reduces the packet error rate and packet retransmission count by 49.8% (error clusters arrival rate, $\lambda = 0.001$ (*/ms*)) and 49.73% ($\lambda =$

0.001 (*/ms*)), respectively.   Moreover, the proposed DMZ HO scheme outperforms an existing overlapping zones (OLZ) scheme. It reduces channel occupation time by 89.3% compared to the OLZ scheme when the HO arrival rate, µ, is 1 (*/sec*). In addition, the proposed DMZ HO scheme consumes less channel bandwidth than the OLZ scheme. The channel idle ratio of the proposed DMZ HO scheme is 89.3% (µ = 1, *PDU-offset* = 10) larger than that of the OLZ scheme. Therefore, the proposed DMZ HO scheme is more cost-effective than the OLZ scheme and is thus very feasible for interactive TV (ITV) applications.

4.1 Proposed DMZ HO

The level-2 frame-offset coordination requires the data transmissions between any two adjacent MBS zones are synchronized so that it can provide HO MSs with the continuity of data reception during inter-MBS HO [23]. Therefore, during inter-MBS zone HO, providing data continuity for HO MSs is equivalent to support the level-2 frame-offset coordination. In this section, we propose a DMZ framework to support level-2 frame-offset coordination for inter-MBS zone HO. Based on the proposed DMZ framework, a seamless DMZ HO scheme is proposed to resolve the positive PDU-O value problem between any two adjacent MBS zones so as to support HO MSs for data continuity during inter-MBS zone HO.

4.1.1 Aggregating MBS Sync Rules and MBS Payload

For transmission synchronization, the MBS sync rules distribute the transmission information of corresponding MBS payloads.   Therefore, any packet error of MBS payloads or their associated sync rules during the Accumulation Period should be recovered within the following Recovery Period. The Period should be long enough to finish both sync rule and data path recovery procedures. A longer Recovery Period means a larger size of a packet buffer pool required, and

it results in longer transmission latency. Reducing the packet loss probability of both MBS payloads and their associated sync rules can lead to lower transmission latency and a smaller size of the packet buffer pool. In this Chapter, we propose an in-frame control (IFC) scheme that aggregates the MBS payload and its associated MBS sync rules. In contrast to transmitting the MBS payload and its associated MBS sync rules separately, binding both the MBS payload and its associated sync rules together can reduce the probability of starting recovery procedures. A packet aggregating an MBS payload and its associated sync rules is termed as an *IFC packet*. By using IFC packets instead of individual MBS payload packets and sync rules, we can shorten the packet transmission latency and reduce the size of the packet buffer pool.
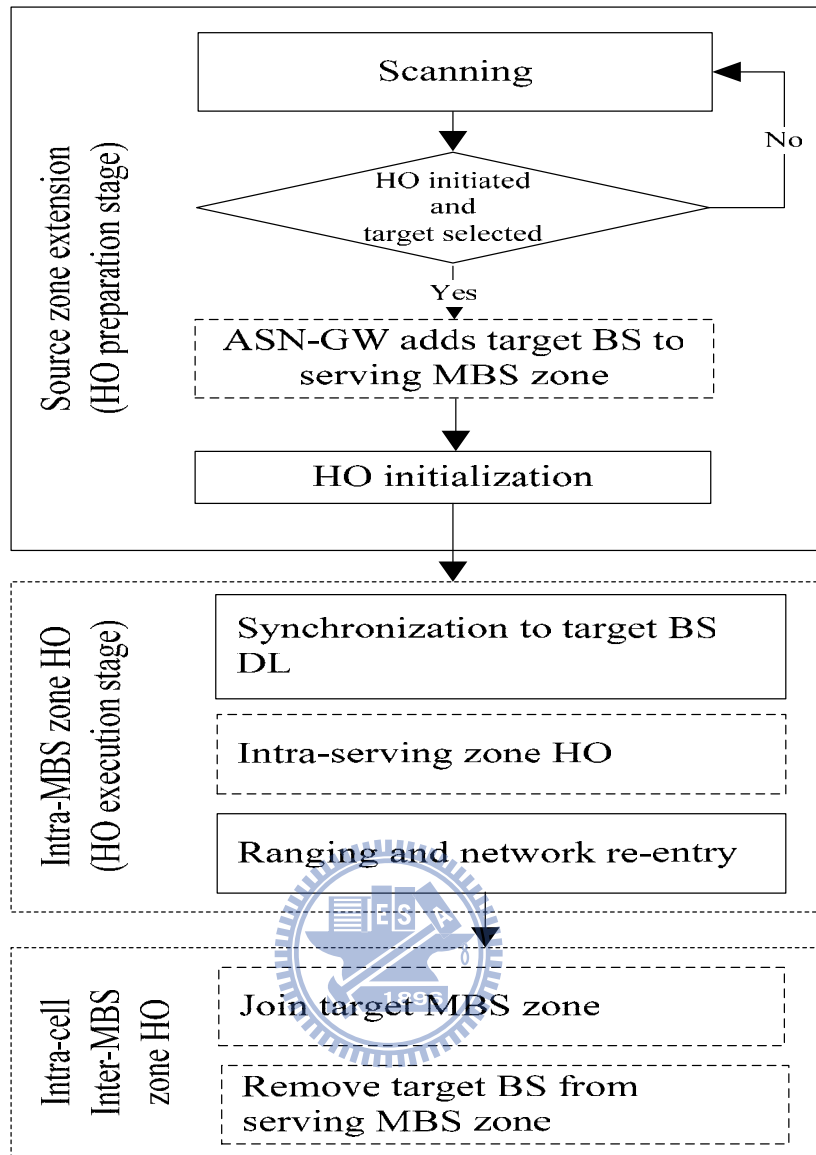
Fig. 4.1: Proposed DMZ HO.

4.1.2 Dynamically scaling up the MBS zone

The HO process of the IEEE 802.16-2009 [1] can be functionally divided into two stages: *HO preparation* and *HO execution*. In the HO preparation stage, an MS selects a target BS and then proceeds with HO initialization. In the HO execution stage, the MS performs downlink synchronization, ranging and network re-entry; this stage starts actual HO. Based on the HO process, we propose a DMZ framework to support level-2 frame-offset coordination. The proposed DMZ framework dynamically overlaps the serving and target zones to resolve data

discontinuity. After the HO is completed, the serving and target zones are reverted to non-overlapping. Without loss of generality, we assume that each MBS zone is a single-BS MBS zone. Fig. 4.1 shows an overview of the proposed DMZ HO. In the proposed DMZ framework, the inter-MBS zone HO is divided into three phases: *source zone extension*, *intra-MBS zone HO*, and *intra-cell inter-MBS zone HO*. The source zone extension and intra-MBS zone HO operate in the HO preparation stage and HO execution stage respectively. The intra-cell inter-MBS zone HO is started when the MS resolves the data discontinuity between the serving and target MBS zones. Assume that the MS is now served by the serving MBS zone. In the HO preparation stage, the serving ASN-GW performs the source zone extension by adding the target BS to the serving MBS zone. After the target BS joins the serving MBS zone, the serving MBS zone becomes a two-BS MBS zone, and the serving IFC packets are delivered to the serving BS and the target BS. Then, in the HO execution stage, an MS treats the HO within the serving MBS zone as an intra-MBS zone HO. In the HO execution stage, the MS handovers to the target BS and then joins the target MBS zone. As to the serving MBS zone, the MS performs an intra-MBS zone HO to switch the MBS services from the serving BS to the target BS. In the intra-MBS zone HO, the frame-level coordination is used for data synchronization. At the beginning of the intra-cell inter-MBS zone HO, the MS not only belongs to the serving MBS zone but also join the target MBS zone. Through the target BS, the MS concurrently receives the MBS payloads from both the serving MBS zone and the target MBS zone until redundant MBS payloads are received from either zone. Note that in the case of negative PDU-O value, the MS will immediately detect redundant MBS payloads from the target MBS zone. On the contrary, in the case of positive PDU-O value, the MS will not detect redundant MBS payloads until all the PDU-O packets are received from the source MBS zone. After detecting redundant MBS payloads, the MS informs the target BS to terminate the serving zone service, which completes the intra-cell inter-MBZ zone HO.
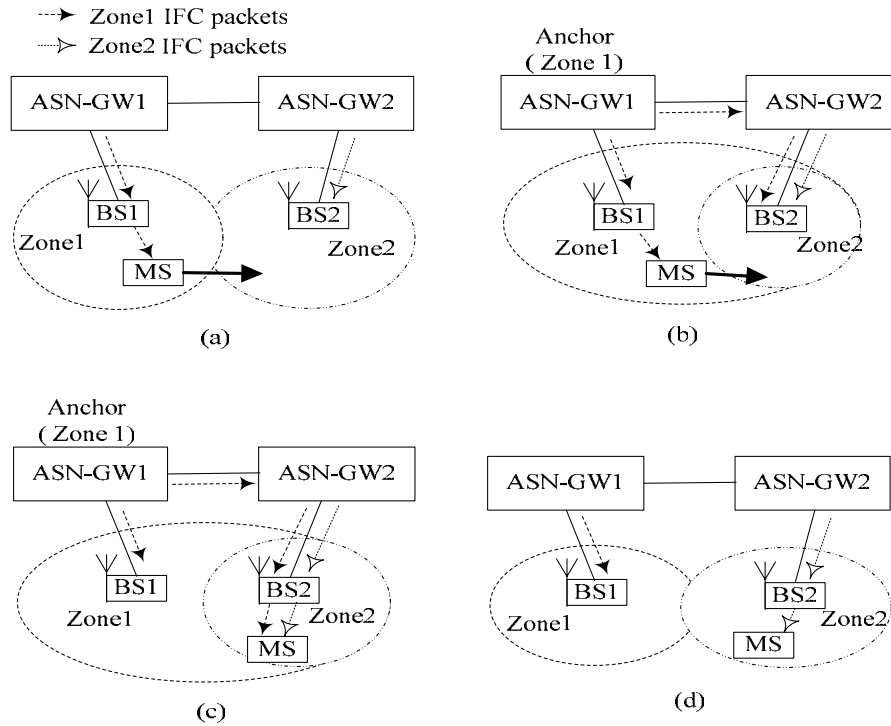
Fig. 4.2: An illustration of the proposed DMZ HO. (a) An MS moves from MBS zone1 to MBS zone2. (b) Perform source zone extension to add BS2 to zone1. (c) The MS handovers to BS2 by performing intra-MBS zone1 HO, and then the MS also joins zone2. (d) The MS performs intra-cell inter-MBS zone HO in BS2, and then BS2 is removed from zone1.

An illustration of the proposed DMZ HO is given in Fig. 4.2. Fig. 4.2(a) shows that both MBS zone1 and MBS zone2 provide the same MBS service. ASN-GW1 and ASN-GW2 are in charge of zone1 and zone2, respectively. When the MS in BS1 decides to handover to BS2, ASN-GW1 adds BS2 to zone1. Fig. 4.2(b) performs the source zone extension so that BS2 joins zone1, and ASN-GW1 is the anchor ASN-GW of zone1. At this moment, BS2 provides both zone1 service and zone2 service. The zone1 IFC packets are issued from the ASN-GW1 (anchor) to both BS1 and BS2. Moreover, BS2, providing zone2 service, still keeps receiving IFC packets from zone2. Fig. 4.2(c) shows that the MS performs intra-MBS zone HO in the zone1, and it also joins the zone2. The MS, simultaneously receiving MBS bursts from both zone1 and zone2

through BS2, checks for redundant payloads by inspecting the sequence number of MBS payloads from both zones. Upon receiving redundant payloads, the MS issues the intra-cell inter-MBS zone HO by signaling BS2 to terminate the zone1 service and then receiving MBS service dedicated from zone2. Fig. 4.2(d) shows that the MS completes the intra-cell inter-MBS zone HO, and the target BS is removed from zone1.
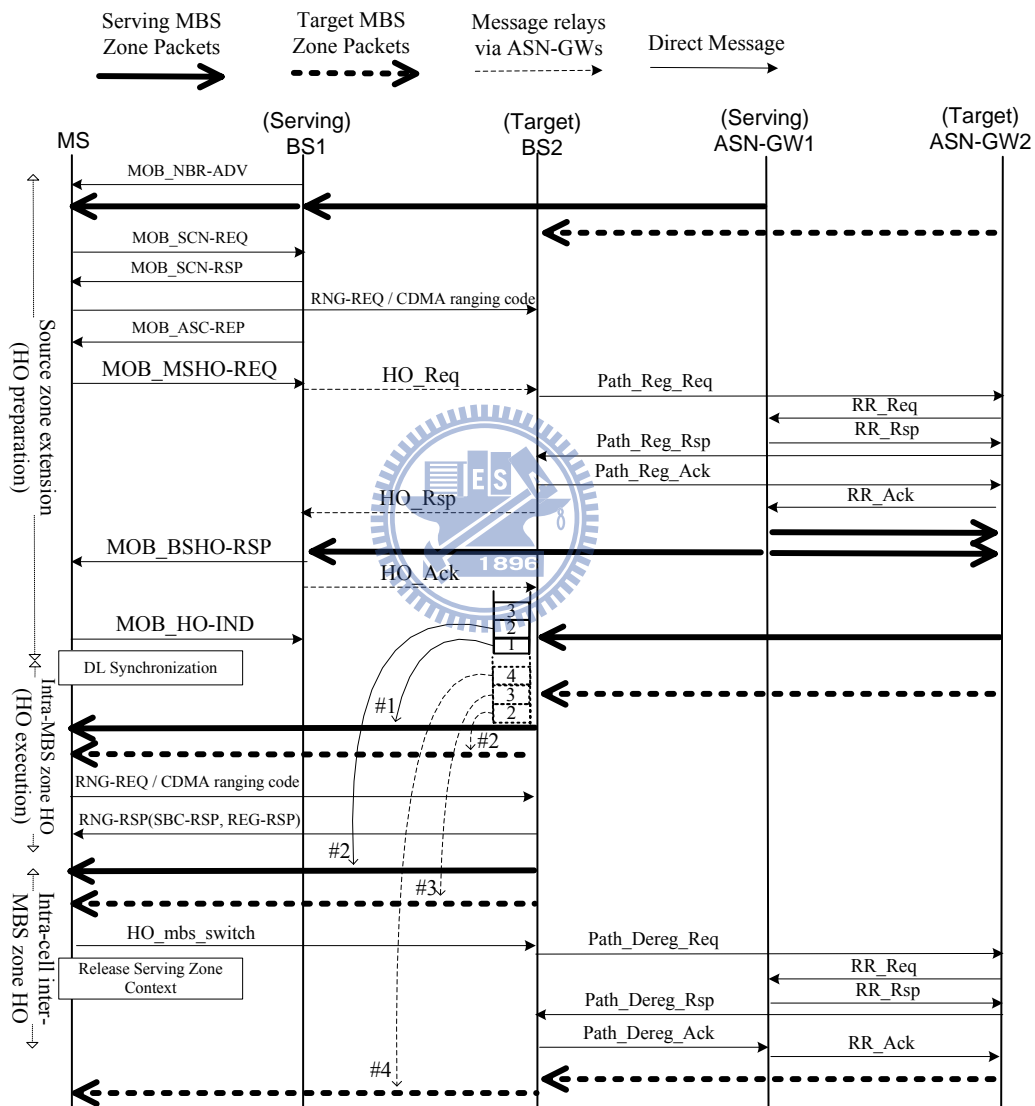

Fig. 4.3: MSC of the proposed DMZ HO.

Based on Fig. 4.2, Fig. 4.3 shows the detailed message sequence chart (MSC) of the proposed DMZ HO. BS1 and ASN-GW1 are the serving BS and serving ASN-GW, respectively. BS2 and ASN-GW2 are the target BS and target ASN-GW, respectively. The bold lines and dashed bold lines show the MBS IFC packet flows to the serving MBS zone and target MBS zone, respectively. The dashed thin lines are management messages. The solid thin lines are sent directly from source to destination, and the dashed thin lines sent from source to destination are relayed via the two ASN-GWs. The management messages termed with all capital letters are the MAC management messages defined in the IEEE 802.16-2009 [1], and the other management messages termed with leading capital letters and followed by low case letters are the control messages defined in the WiMAX standard [23]. The proposed seamless inter-MBS zone DMZ HO scheme based on the DMZ framework is detailed as follows (see Fig. 4.3):

1) The MS gets adjacent BSs information from the received MOB_NBR-ADV message. The MCID pre-allocation information in the MOB_NBR-ADV message provides MCID mappings between the serving MBS zone and adjacent MBS zones. In the HO preparation stage, the MS starts scanning by issuing an MOB_SCN-REQ message to request a group of time intervals from the serving BS (BS1), and the serving BS grants the time intervals by replying an MOB_SCN-RSP message.   Within the time intervals, the MS associates to BS2, and eventually the serving BS sends association results to the MS by sending an MOB_ASC-REP message.

2) The MS issues an MOB_MSHO-REQ message to notify that BS2 is the HO target. The serving BS sends an HO_Req message to the target BS (BS2). The HO_Req message which carries MBS service flow information will enable the target BS to start creating an MBS service flow to the serving ASN-GW1.

3) After inspecting the information in the HO_Req, the target BS initiates a dynamic service flow creation for the MBS. By exchanging the Path_Reg_Req/Rsp/Ack and

RR_Req/Rsp/Ack messages, the data path between the serving ASN-GW1 and the target BS is created, and then IFC packets from the serving MBS zone are delivered to the target BS. At the end of the HO preparation stage, both the serving and target zones are overlapped at the target BS.

4) In the HO execution stage, the MS synchronizes to the target BS DL. By obtaining the MCID pre-allocation information from the MOB_NBR-ADV message, the MS joins the target MBS zone and is able to receive both the serving and target MBS packets simultaneously before starting the ranging and network re-entry. As shown in Fig. 4.3, after DL synchronization, the MS receives packet #1 from the serving zone and packet #2 from the target zone before the RNG-RSP message is received.

5) After completing the ranging and network re-entry, the MS keeps receiving MBS bursts from both the serving zone and target zone until a redundant MBS payload is found. Note that the redundancy check can be done by checking the sequence number, such as the transport layer sequence number in the reassembled MBS bursts. Once a redundant MBS payload is found, the MS issues HO_mbs_switch to notify the target BS that the MS will leave the serving MBS zone. As shown in Fig. 4.3, the MS receives a packet with sequence number #2 from the target zone before issuing an RNG-REQ message. After that, another packet with the same sequence number #2 is also received from the serving zone. The MS assures that data discontinuity is resolved and then issues HO_mbs_switch to finalize the inter-MBS zone HO. Note that the HO case shown in Fig. 4.3 assumes that the PDU-O value is 1 between the source and target zones.

6) Any redundant MBS payload from the serving or target zone indicates that the HO has resolved the potential loss problem of MBS payloads. After receiving an HO_mbs_switch message, the target BS might delete the service flow by exchanging Path_Dereg_Req/Rsp/Ack and RR_Req/Rsp/Ack messages. Note that path deregistration

from the serving zone is issued only when there is no subsequent ongoing HOs. After this procedure, the target BS leaves the serving zone, and now the service and target zones are non-overlapped.

4.2 Analytic Model

In this section, we will analyze the performance of the proposed IFC scheme and DMZ HO scheme. The proposed IFC scheme focuses on preventing the BS from entering the recovery procedures. Therefore, the packet error rate and packet retransmission count are two key performance metrics. In section 4.2.1, we analyze the packet error rate and the expectation of the packet retransmission count. In addition, the proposed DMZ HO scheme supports data continuity by dynamically allocating a channel during HO to transport PDU-O between the serving MBS zone and the target MBS zone. The bandwidth overhead of an HO can be reflected by the usage of the dynamic allocated channel. In section 4.2.2, we analyze the channel usage in terms of the expectation of the channel occupation time.
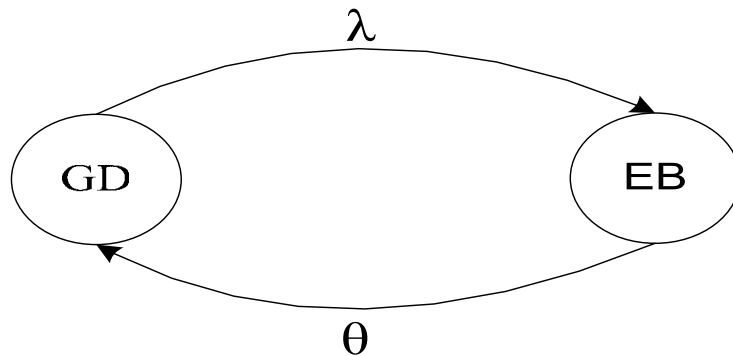

Fig. 4.4: State transition diagram of the Markov process for a link.

4.2.1 Derivations of the Packet Error Rate and the Expectation of the Packet Retransmission Count

To analyze the packet retransmission count, we assume the arrivals of physical impairments in a link are a Poisson process [26]. A physical impairment results in a period of incorrect transmission, which was termed as an error cluster. Depending on the nature of physical impairments, the durations of error clusters also have a probability distribution [26]. In addition, an error only occurs within an error cluster, and the last bit of each error cluster is always an error bit [26].

We model a link with errors by the M/M/1/1 queuing model and assume a link is either in the good state (GD) or in the error burst (EB) state [26]. The GD state denotes a link is out of error clusters durations, and the EB state denotes a link is within the periods of error clusters. Fig. 4.4 shows the state transition of the Markov process for a link. Assume that the arrivals of error clusters are a Poisson arrival process with arrival rate λ, and θ denote the departure rate of the EB state. Thus, the inter-arrival time is exponentially distributed with the probability density function [17][18][21].

$$f(t) = \lambda e^{-\lambda t} \qquad t \geq 0 \tag{1}$$

Let δ denote a random variable to represent the duration of an error cluster. Assume that δ has the mixed Erlang distribution with the probability density function

$$f_\delta(t) = \sum_{i=1}^{I} c_i \frac{(\phi_i t)^{r_i - 1}}{(r_i - 1)!} \phi_i e^{-\phi_i t} \tag{2}$$

where

$$\sum_{i=1}^{I} c_i = 1$$

69

Note that in Eq. (2), I, c_i, r_i and ϕ_i determines the shape and scale of the distribution [18].

We select the mixed Erlang distribution because it has been proven that it can well approximate

to many other distributions [17] [18] [21]. Thus, the expectation of δ is expressed as

$$E\left(\delta\right)=\int_{t=0}^{\infty}f_{\delta}\left(t\right)t\,dt$$

(3)

$$=\sum_{i=1}^{I}\frac{c_i\phi_i^{r_i}}{\left(r_i-1\right)!}\int_{t=0}^{\infty}t^{r_i}e^{-\phi_it}\,dt$$

By Laplace transform, we get

$$E\left(\delta\right)=\sum_{i=1}^{I}c_i\left(\frac{r_i}{\phi_i}\right)$$

(4)

Then, the departure rate, θ, can be expressed as $\theta = 1/E(\delta)$. Furthermore, we assume the

expectation of inter-arrival time between any two continuous error clusters is much longer than

the expectation of an error cluster duration so that the overlapping probability of two adjacent

error clusters can be ignored [26]. Let the state probabilities of GD and EB be π_0 and π_1,

respectively. From [20], we get

$$\pi_0=\left(1+\lambda/\theta\right)^{-1}$$

(5)

and

$$\pi_1=\left(\lambda/\theta\right)\left(1+\lambda/\theta\right)^{-1}$$

(6)

Since the error cluster duration and the EB state probability are significantly small, the

probability of transmitting a packet within the EB state without errors can be neglected. Thus,

the packet error rate (PER) can be expressed as

$$PER=\pi_0\int_{t=0}^{t_p}f\left(t\right)dt+\pi_1$$

(7)

$$=\pi_0\left(-e^{-\lambda t}\Big|_{t=0}^{t_p}\right)+\pi_1$$

$$= 1 - \pi_0 e^{-\lambda t_p}$$

where t_p is the packet transmission duration.

Let σ denote the packet retransmission count for successfully delivering a packet to its destination. Therefore, the expectation of σ is expressed as follows:

$$E(\sigma) = \sum_{n=1}^{\infty} n \left(1 - \pi_0 e^{-\lambda t_p}\right)^{n-1} \left(\pi_0 e^{-\lambda t_p}\right) - 1$$

(8)

4.2.2 Derivation of the Expectation of the Channel Occupation Time

After the target BS is added to the source MBS zone in the source zone extension phrase, it allocates a channel to deliver the PDU-O packets between two adjacent MBS zones. For this, we will analyze the expectation of the channel occupation time in this section. Fig. 4.5 shows a timing diagram of HO arrivals to a BS.
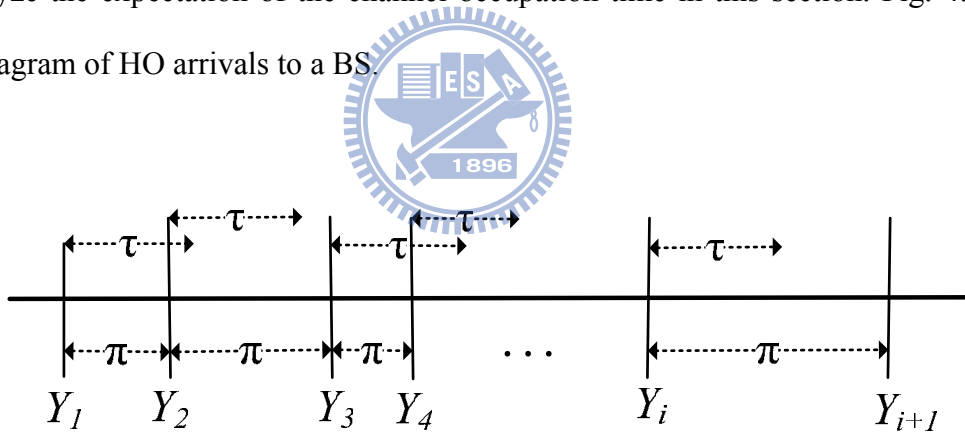
Fig. 4.5: Timing diagram of HO arrivals to a BS.

Assume that the arrivals of HO MSs from an adjacent MBS zone into a BS are a Poisson arrival process with arrival rate μ. Y_i denote an event of the ith arrival MS, and π is the interarrival time between two adjacent arrivals. τ will be defined later. Thus, the interarrival time is exponentially distributed with the probability density function

$$f_\pi(t) = \mu e^{-\mu t} \qquad t \geq 0$$

(9)

Note that the target BS allocates a channel to deliver PDU-O packets. Thus, the bandwidth overhead of the proposed DMZ HO can be represented as the expectation of channel occupation time. Let α and β be random variables to represent the processing times of DL synchronization and the HO_mbs_switch message (see Fig. 4.3), respectively. Assume that both α and β have the mixed Erlang distributions with the following density functions [18] [21]

$$f_\alpha(t) = \sum_{i=1}^{I} a_i \frac{(v_i t)^{p_i - 1}}{(p_i - 1)!} v_i e^{-v_i t}$$

(10)

$$f_\beta(t) = \sum_{j=1}^{J} b_j \frac{(\phi_j t)^{q_j - 1}}{(q_j - 1)!} \phi_j e^{-\phi_j t}$$

(11)

where

$$\sum_{i=1}^{I} a_i = 1 \text{ and } \sum_{j=1}^{J} b_j = 1$$

The corresponding Laplace transforms are shown as follows:

$$f_\alpha^*(s) = \sum_{i=1}^{I} a_i \left(\frac{v_i}{s + v_i} \right)^{p_i}$$

(12)

$$f_\beta^*(s) = \sum_{j=1}^{J} b_j \left(\frac{\phi_j}{s + \phi_j} \right)^{q_j}$$

(13)

Remind that the MS receives MBS packets from the source MBS zone right after DL synchronization (see Fig. 4.3). Let γ_n denote the nth packet arriving at the MS in the dynamic MBS zone in the period $[0, t]$. Assume γ_n has an Erlang distribution with the probability density function

$$f_{\gamma_n}(t) = \frac{(\rho t)^{n-1}}{(n-1)!} \rho e^{-\rho t}$$

(14)

And the Laplace transform for γ_n is

$$f_{\gamma_n}^*(s) = \left(\frac{\rho}{s+\rho}\right)^n$$

(15)

Let τ denote the channel occupation time allocated by the dynamic MBS zone for an MS to deliver PDU-O packets. We have

$$\tau = \begin{cases} \alpha + \gamma_n + \beta & \pi \geq \alpha + \gamma_n + \beta \\ \pi & \pi < \alpha + \gamma_n + \beta \end{cases}$$

(16)

Note that we assume the MS is capable of sending the HO_mbs_switch message before the ranging and network re-entry is completed [27]. Let $T_c = \alpha + \gamma_n + \beta$. Therefore, the expectation of the channel occupation time for an MS can be expressed as

$$\begin{aligned}
E(\tau) &= \int_{T=0}^{\infty} f_{T_c}(T) \int_{t=T}^{\infty} f_\pi(t) T dt dT \quad + \\
&\quad \int_{T=0}^{\infty} f_{T_c}(T) \int_{t=0}^{T} f_\pi(t) t dt dT \\
&= \int_{T=0}^{\infty} f_{T_c}(T) T e^{-\mu T} dT \quad + \\
&\quad \int_{T=0}^{\infty} f_{T_c}(T)\left(\mu^{-1} - \mu^{-1} e^{-\mu T} - T e^{-\mu T}\right) dT \\
&= \mu^{-1}\left[f_{T_c}^*(s)\big|_{s=0}\right] - \mu^{-1}\left[f_{T_c}^*(s)\big|_{s=\mu}\right]
\end{aligned}$$

(17)

Since $T_c = \alpha + \gamma_n + \beta$ and $f_{T_c}(t)$ denotes the probability density function of T_c, by applying the convolution property, its Laplace transform, $f_{T_c}^*(s)$, is as follows

$$f_{T_c}^* = f_\alpha^* f_{\gamma_n}^* f_\beta^*$$

(18)

Substitute, $f_{T_c}^*(s)$, into Eq. (17), we get

$$E(\tau) = \mu^{-1}\left\{ \begin{aligned} &1 - \left[\sum_{i=1}^{I} a_i\left(\frac{v_i}{\mu+v_i}\right)^{p_i}\right] \\ &\times \left(\frac{\rho}{\mu+\rho}\right)^n \left[\sum_{j=1}^{J} b_j\left(\frac{\phi_j}{\mu+\phi_j}\right)^{q_j}\right] \end{aligned} \right\}$$

(19)

73

4.3 Performance Evaluation

Based on the analytic model derived in the last section, we present analytic results of the proposed IFC and DMZ HO schemes. In section 4.3.1, the proposed IFC scheme and the original WiMAX scheme are compared in terms of packet error rate and packet retransmission count. In section 4.3.2, we compare the channel usage in terms of channel occupation time and channel idle ratio between the proposed DMZ HO scheme and the existing OLZ scheme [25].

TABLE 4.1: PARAMETER SETTINGS FOR PERFORMANCE EVALUATION.

PARAMETER	VALUE	
Backhaul network bandwidth	1 Gbps	
δ	$c_1 = c_2 = 0.5$ $\phi_1 = 2, \phi_2 = 3$ (/ms)	
MBS payload (MP)	MP_512B (512 bytes data payload)	MP_1024B (1024 bytes data payload)
	Packet header overhead: 70 bytes	
Sync rule (SR)	97 bytes payload for MP_512B	133 bytes payload for MP_1024B
	Packet header overhead: 50 bytes	
IFC packet	609 bytes payload (MP_512B + SR)	1157 bytes payload (MP_1024B + SR)
	Packet header overhead: 70 bytes	

4.3.1 Comparison between the Proposed IFC Scheme and the Original WiMAX Scheme

In this section, we evaluate the performance of the proposed IFC scheme in terms of the packet error rate and the expectation of packet retransmission count. Without loss generality, we assume the random variable, δ, is a mixed Erlang-2 distribution [18] [21], and the coefficients for δ were set to $c_1 = c_2 = 0.5$ [18]. Furthermore, we assume the MBS payload only has an associated sync rule. Table 4.1 shows the parameter settings for performance evaluation. By Eq.(7), Fig. 4.6 compares the packet error rates of the proposed IFC scheme and the original WiMAX scheme. We assume the MBS payload length is 512 bytes, and its associated sync rule payload is 97 bytes, which carries three fragmentations information. Thus, the payload length of the proposed IFC packet is 609 bytes, which is formed by aggregating the MBS payload and its associated sync rule. Due to long packet length of the IFC packet, we found that the packet error rate of the IFC packet is a little higher than that of the MBS payload or the sync rule. Owing to figure resolution, some curves in Fig. 4.6 are almost overlapped. Therefore, we show three sets of sample data to reveal the relations among curves. Note that the original WiMAX scheme treats the packet errors as any errors from the MBS payload or from the associated sync rule. In Fig. 4.6, it shows that the proposed IFC scheme reduces the packet error rate by 49.8% ($\lambda = 0.001$), 35.0% ($\lambda = 1$), and 0.68% ($\lambda = 100$) compared to the original WiMAX scheme. In addition, Fig. 4.6 also shows the packet error rates of the MBS payload and the sync rule. We found that the IFC packet only has a slightly higher packet error rate than that of the MBS payload or the sync rule, but it has much lower packet error rate than that of the original WiMAX scheme. By Eq. (8), we compare the packet retransmission count between the proposed IFC scheme and the original WiMAX scheme. In Fig. 4.7, it shows that the proposed IFC scheme reduces the packet retransmission count by 49.73% ($\lambda = 0.001$, MP_1024B), 49.69% ($\lambda = 0.1$,

MP_1024B), and 47.35% ($\lambda = 10$, MP_1024B) compared to the original WiMAX scheme. Moreover, a smaller MBS payload length resulted in a lower packet retransmission count than a larger MBS payload length. Again, we also show three sets of sample data to reveal the relations among curves.
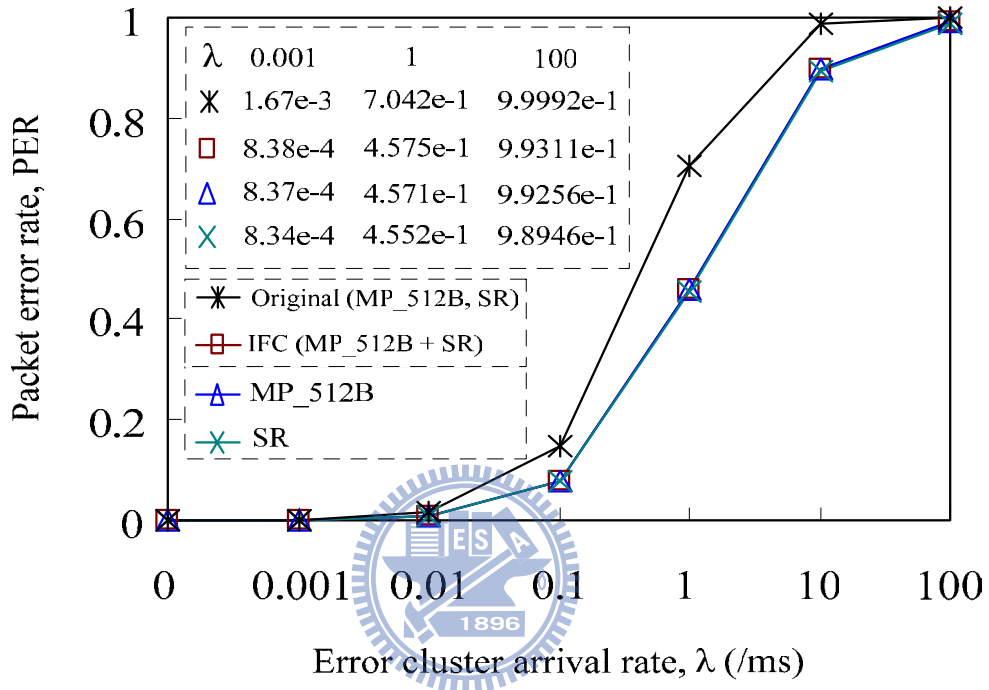

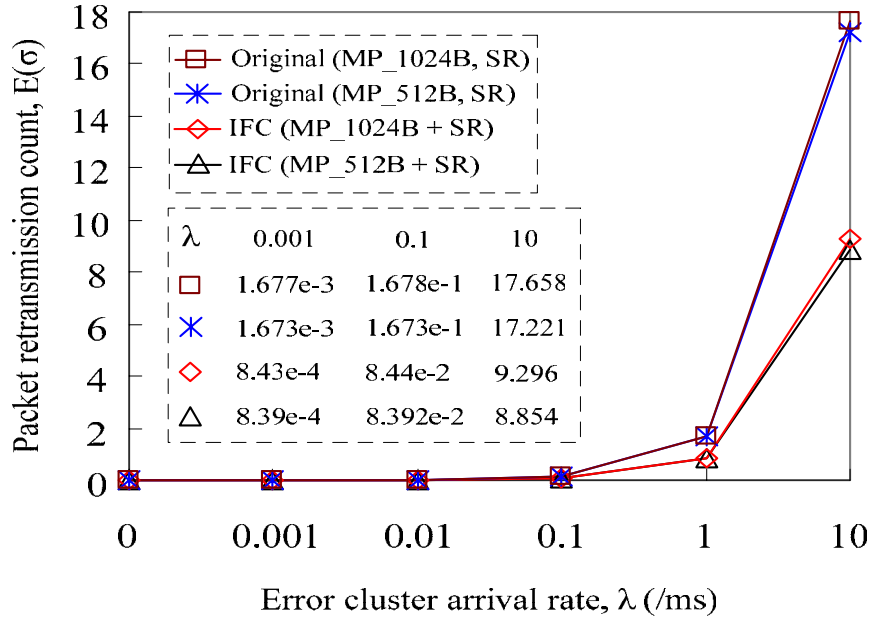Fig. 4.6: Packet error rate versus error cluster arrival rate.

Fig. 4.7: Packet retransmission count versus error cluster arrival rate.

4.3.2 Comparison between the Proposed DMZ HO and the OLZ Scheme

To evaluate bandwidth overhead of the proposed DMZ HO scheme with respect to the OLZ scheme [25], we first compare the channel occupation time. By Eq. (19), Fig. 4.8 shows the expectation of channel occupation time with respect to the HO arrival rate. We found that when the HO arrival rate increases, the expectation of channel occupation time of an HO decreases. It is because the overlapped HO MSs share the allocated channel during the HO execution stage. We observed that the proposed DMZ HO scheme has a lower channel occupation time than the OLZ scheme, especially at a low HO arrival rate setting. This is because the proposed DMZ HO scheme dynamically allocates a channel only to deliver the PDU-O packets. The $E(\tau)$'s of both OLZ and DMZ schemes become gradually close when the HO arrival rate increases. As shown in Fig. 4.8, the proposed DMZ HO scheme outperforms the OLZ scheme by 89.3% ($\mu = 1$, PDU-O = 10) and 3.75e-3% ($\mu = 150$, PDU-O = 10) in terms of channel occupation time. The

DMZ HO scheme with a higher PDU-O has a larger $E(\tau)$ than that with a lower PDU-O. It results from that a higher PDU-O occupies more channel time to receive PDU-O packets. With different HO arrival rates, μ, we investigate the channel idle ratio of the allocated channel in the target BS. The channel idle ratio, computed as $(1 - \mu E(\tau))*100\%$, is defined as the channel idle percentage that is able to be used by other services. Fig. 4.9 shows the relationship between channel idle ratio and PDU-O under different μ. The proposed DMZ HO scheme is more cost-effective than the OLZ scheme because the channel idle ratio of the proposed DMZ HO scheme is larger than that of the OLZ scheme. For example, the channel idle ratios of the DMZ HO scheme are 89.3% ($\mu = 1$, PDU-O = 10) and 34.4% ($\mu = 10$, PDU-O = 10) larger than those of the OLZ scheme. Compared with the OLZ scheme, which fully uses the allocated channel bandwidth, the proposed DMZ HO scheme only dynamically allocate a channel to resolve the data discontinuity between the serving and target MBS zones. Note that the channel idle ratio of the OLZ is always zero because of full utilization of the allocated channel. The proposed DMZ HO scheme with a small μ setting can free the allocated channel more than that with a large μ setting. Remind that the channel idle ratio is inversely correlated to the PDU-O. It is resulted from that, with a larger PDU-O, each MS requires more channel bandwidth to receive PDU-O packets.
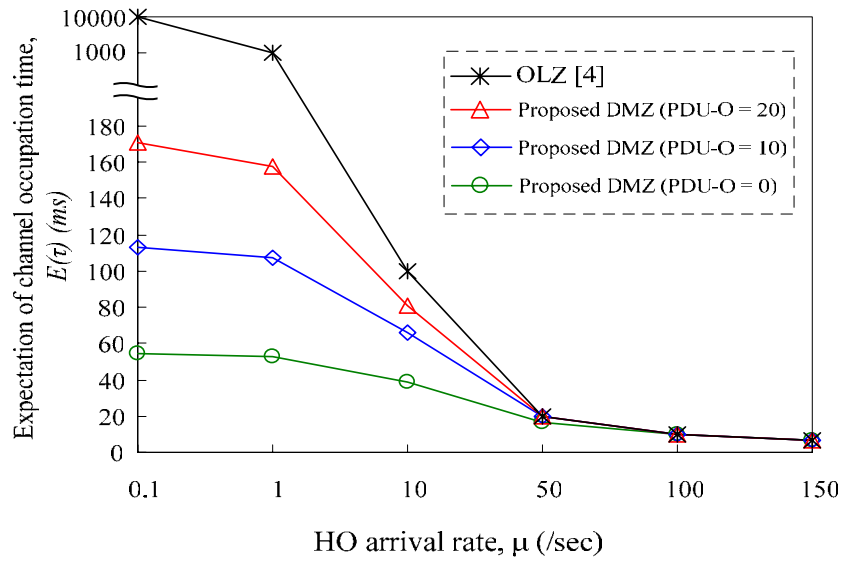
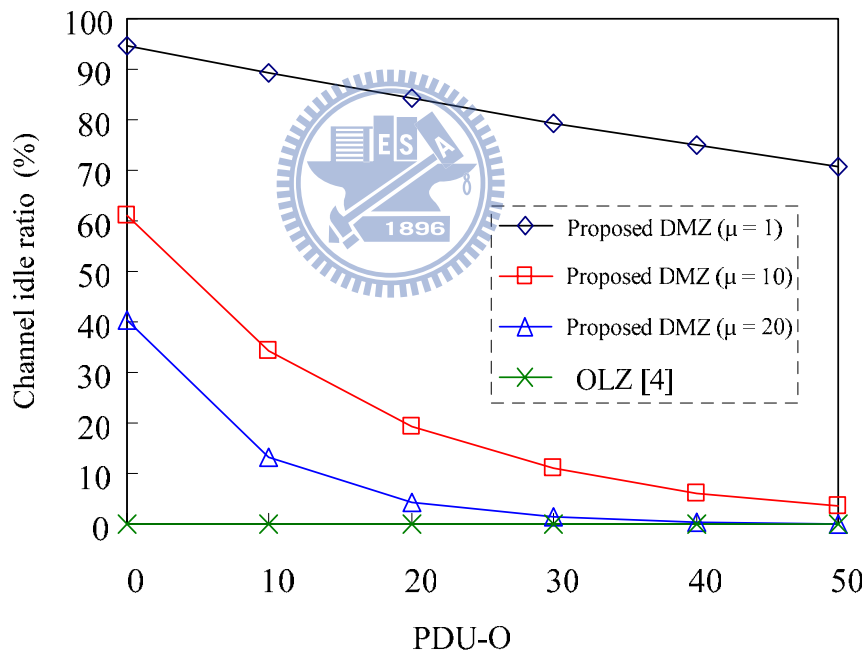Fig. 4.8: Channel occupation time versus HO arrival rate.

Fig. 4.9: Channel idle ratio versus PDU-O.

Chapter 5

Conclusions and Future Work

5.1 Concluding Remarks

In Chapter 3, we have presented a novel IEEE 802.16e network architecture. Based on this architecture, a network-assisted fast handover (NFHO) scheme has been proposed to shorten the service disruption time during HO. Since the proposed NFHO scheme resolves the transport CIDs assignment and UL synchronization issues before the HO ranging, the UL/DL data transmission is able to be restarted before the MS proceeds to the HO ranging. In this scheme, DL packets are bicast to the target BS as well as the serving BS before breaking the connection with the serving BS. In addition, we have also developed an analytic model to evaluate the expected number of buffered packets, the packet loss probability and the service disruption time. Based on the analytic model, we can also evaluate the relationship among the packet loss probability, packet arrival rate, number of concurrent HO MSs, and the size of the HO packet buffer pool. Performance evaluation results have shown that the proposed NFHO scheme reduces the DL service disruption time by 75% compared to the IEEE 802.16e hard HO scheme. It also reduces the UL service disruption time by 55.6% compared to Jiao et al. and by 75% compared to both Choi et al. and the IEEE 802.16e hard HO scheme. In summary, the NFHO scheme has the best performance in terms of the expected number of buffered packets, packet loss probability and service disruption time among existing hard HO schemes for the IEEE 802.16e. The derived analytic model can also be integrated to an admission control policy to provide proper QoS to ongoing HO MSs.

In Chapter 4, we have also presented an in-frame control (IFC) scheme that aggregates an

MBS PDU and its associated sync rules. The proposed IFC scheme can reduce the packet error rate and packet retransmission count of MBS services. By reducing the packet error rate, we can decrease the probability of entering the recovery procedure that enlarges the packet transmission latency and the packet buffer pool requirement. In addition, we have also presented a dynamic MBS zone (DMZ) framework for inter-MBS zone HO. Based on this DMZ framework, a DMZ HO scheme has been proposed to support data continuity and achieve cost-effectiveness. In addition, an analytic model has been developed to evaluate the proposed IFC and DMZ HO schemes. Performance evaluation results have shown that the proposed IFC scheme outperforms the original WiMAX scheme in terms of packet error rate by 49.8% when the error clusters arrival rate is 0.001 (*/ms*), and the proposed DMZ HO scheme outperforms the OLZ scheme in terms of channel occupation time by 89.3% when the HO arrival rate is 1 (*/sec*). In summary, the proposed IFC scheme has the better performance in terms of packet error rate and packet retransmission count compared to the original WiMAX scheme. In addition, the proposed the DMZ HO scheme can provide data continuity during inter-MBS HO with much less bandwidth overhead compared to the OLZ scheme, and thus is very feasible for interactive TV (ITV) applications. For future work, the proposed DMZ framework can also be used for seamless MBS zones coalescence or MBS zone division (or separation) for efficient use of radio resources.

5.2 Future Work

Based on the research results presented in this dissertation, the following directions are worth to investigate in the future.

- Association in the Cell Reselection stage is used to acquire ranging parameters and service availability information that could expedite the HO Execution procedure. To acquire UL synchronization parameters, we redo association to acquire fresh UL synchronization parameters in the HO Decision and Initiation stage. The decision to renew UL parameters

depends on some factors, such as the difference of DL arrival times since last association, the decay of mean CINR (carrier to interference and noise ratio) since last association, and a refresh timer. Here we simply assume that the MS decides to renew the UL parameters when a refresh timer has expired. However, the refresh timer might not be a precise decision for redoing association. Thus, it deserves to investigate a decision mechanism for redoing association.

- In Chapter 3, we develop an analytic model to analyze packet loss probability during HO. Since the target BS only has limited packet buffers to queue bicast packets during HO, bicast packets arrived at the target BS are dropped if there is no available packet buffer. Therefore, the analytic model can be integrated into an admission control policy to guarantee proper QoS for ongoing HO MSs. It is an issue deserved to study for applying the analytic results for HO MSs admission control.

- In Chapter 4, we propose a dynamic MBS zone (DMZ) framework that can provide data continuity between any two adjacent MBS zones. The DMZ framework can dynamically extend the source MBS zone and perform intra-MBS zone HO and intra-cell inter-MBS zone HO. Therefore, for resource management, the DMZ framework can be used for seamless MBS zones coalescence or MBS zone division. In a WiMAX network that supports dynamic MBS zone configuration needs to handle MBS zones coalescence or MBS zone division. Therefore, applying the DMZ framework to manage the MBS zone configuration is an investigable future work.

Bibliography

[1] *IEEE Standard for Local and Metropolitan Area Networks – Part16: Air Interface for Fixed Broadband Wireless Access Systems*, IEEE Std. 802.16-2004, Oct. 2004.

[2] *IEEE Standard for Local and Metropolitan Area Networks – Part16: Air Interface for Fixed and Mobile Broadband Wireless Access Systems*, IEEE Std. 802.16e-2005, Feb. 2006.

[3] S. Lee, K. Sriram, K. Kim, Y. H. Kim and N. Golmie, "Vertical Handoff Decision Algorithms for Providing Optimized Performance in Heterogeneous Wireless Networks," *IEEE Trans. Veh. Technol.*, vol. 58, no. 2, pp. 865-881, Feb. 2009.

[4] B.-J. Chang and J.-F. Chen, "Cross-Layer-Based Adaptive Vertical Handoff with Predictive RSS in Heterogeneous Wireless Networks," *IEEE Trans. Veh. Technol.*, vol. 57, no. 6, pp. 3679-3692, Nov. 2008.

[5] Y.-H. Han, H. Jang, J. Choi, B. Park, and J. McNair, "A Cross-Layering Design for IPv6 Fast Handover Support in an IEEE 802.16e Wireless MAN," *IEEE Network*, pp. 54-62, Nov.-Dec. 2007.

[6] J. Park, D.-H. Kwon and Y.-J. Suh, "An Integrated Handover Scheme for Fast Mobile IPv6 over IEEE 802.16e Systems," in *Proc. IEEE VTC*, pp.1-5, Sept. 2006.

[7] Y.-W. Chen and F.-Y. Hsieh, "A Cross Layer Design for Handoff in 802.16e Network with IPv6 Mobility," in *Proc. IEEE Wireless Communications and Networking Conference*, pp. 3847-3851, Mar. 2007.

[8] Y.-S. Chen, K.-L. Chiu, K.-L. Wu and T.-Y. Juang, "A Cross-Layer Partner-Assisted Handoff Scheme for Hierarchical Mobile IPv6 in IEEE 802.16e," in *Proc. IEEE Wireless Communications and Networking Conference*, pp. 2669-2674, Mar. 2008.

[9] D. H. Lee, K. Kyamakya, and J. P. Umondi, "Fast Handover Algorithm for IEEE 802.16e Broadband Wireless Access System," in *Proc. The 1st International Symposium on Wireless Pervasive Computing*, pp. 1-6, Jan. 2006.

[10] P.-S. Tseng and K.-T. Feng, "A Predictive Movement Based Handover Algorithm for Broadband Wireless Networks," in *Proc. IEEE Wireless Communications and Networking Conference*, pp. 2834-2839, Mar. 2008.

[11] J. Chen, C.-C. Wang and J.-D. Lee, "Pre-Coordination Mechanism for Fast Handover in WIMAX Networks," in *Proc. The 2nd Conference on Wireless Broadband and Ultra Wideband Communications*, Aug. 2007.

[12] O. C. Ozdural and H. Liu, "Mobile Direction Assisted Predictive Base Station Switching for Broadband Wireless Systems," in *Proc. IEEE International Conference on Communications*, pp. 5570-5574, June 2007.

[13] S. Cho, J. Kwun, C. Park, J.-H. Cheon, O.-S. Lee and K. Kim, "Hard Handoff Scheme Exploiting Uplink and Downlink Signals in IEEE 802.16e Systems," in *Proc. IEEE VTC*, pp. 1236-1240, May 2006.

[14] S. Choi, G.-H. Hwang, T. Kwon, A.-R. Lim and D.-H. Cho, "Fast Handover Scheme for Real-Time Downlink Services in IEEE 802.16e BWA System," in *Proc. IEEE VTC*, pp. 2028-2032, May 2005.

[15] W. Jiao, P. Jiang and Y. Ma, "Fast Handover Scheme for Real-Time Application in Mobile WiMAX," in *Proc. IEEE ICC*, pp. 6038-6042, June, 2007.

[16] Y. Xiao, H. Li, Y. Pan, K. Wu and J. Li, "On Optimizing Energy Consumption for Mobile Handsets," *IEEE Trans. Veh. Technol.*, vol. 53, no. 6, pp. 1927-1941, Nov. 2004.

[17] S. Asmussen, *Applied Probability and Queues*. New York: Wiley, 1987.

[18] A.-C. Pang, Y.-B. Lin, H.-M. Tsai, and P. Agrawal, "Serving Radio Network Controller Relocation for UMTS All-IP Network," *IEEE J. Select. Areas Commun.*, vol. 22, no. 4, pp. 617-629, May 2004.

[19] X. Wang, P. Fan, J. Li and Y. Pan, "Modeling and Cost Analysis of Movement-Based Location Management for PCS Networks with HLR/VLR Architecture, General Location Area and Cell Residence Time Distributions," *IEEE Trans. Veh. Technol.*, vol. 57, no. 6, pp. 3815-3831, Nov. 2008.

[20] L. Kleinrock, *Queuing Systems*. New York: Wiley, 1975. vol. 1, Theory.

[21] Y. Fang and I. Chlamtac, "Teletraffic Analysis and Mobility Modeling of PCS Networks," *IEEE Trans. Commun.*, vol. 47, no. 7, pp. 1062-1072, July 1999.

[22] *IEEE Standard for Local and Metropolitan Area Networks – Part16: Air Interface for Fixed Broadband Wireless Access Systems*, IEEE Std. 802.16-2009, May 2009.

[23] *WiMAX Forum Network Architecture – System Requirements, Network Protocols and Architecture for Multicast and Broadcast Services, Dynamic Service Flow Based (MCBCS - DSx),* Rel. 1.5, Ver. 1, Draf. 0, Nov. 2009.

[24] J. H. Lee, S. Pack, T. Kwon and Y. Choi, "Reducing Handover Delay by Location Management in Mobile WiMAX Multicast and Broadcast Services," *IEEE Trans. Veh.*

Technol., vol. 60, pp. 605-617, Feb. 2011.

[25] K.-H. Hu, H.-L. Fu and P. Lin, "Design of Zone Configuration Scheme for Wireless Zone-based Multicast and Broadcast Service," in *Proc. ACM IWCMC*, pp. 178-182, June 2010.

[26] Y.-Y. Wang and C.-C. Lu, "Error Performance Analysis in Concatenated Digital Transmission Systems by Two-Layered Modeling," *IEEE Trans. on Communications*, vol. 43, no. 2/3/4, pp.1356-1364, Feb./March/April 1995.

[27] L.-S. Lee and K. Wang, "Design and Analysis of a Network Assisted Fast Handover Scheme for IEEE 802.16e Networks," *IEEE Trans. Veh. Technol.*, vol. 59, no. 2, Feb. 2010.
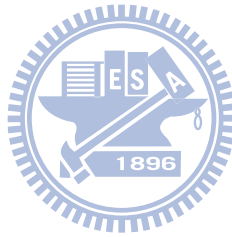
Vita

Lung-Sheng Lee received the M.S. degree in computer and information science from the National Chiao Tung University, Taiwan, in June 1997. He received the Ph.D. degree in computer science and information engineering from the National Chiao Tung University, Taiwan, in January 2012. His research interests include PCS networks, WiMAX networks, and real-time OS.

Publication List

Journal Papers

1. <u>Lung-Sheng Lee</u> and Kuochen Wang, "Design and Analysis of a Network Assisted Fast Handover Scheme for IEEE 802.16e Networks," *IEEE Trans. Veh. Technol.*, vol. 59, no. 2, Feb. 2010.

2. Kuochen Wang and <u>Lon-Sheng Lee</u>, "Design and Analysis of QoS Supported Frequent Handover Schemes in Micro-Cellular ATM Networks," *IEEE Trans. Veh. Technol.*, Vol. 50, Issue 4, pp. 942-953, July 2001.

Journal Papers Submitted

1. <u>Lung-Sheng Lee</u> and Kuochen Wang, "A Dynamic MBS Zone Framework for Cost-Effective Inter-MBS Zone Handover in WiMAX Networks," (Submitted to *IEEE Trans. Veh. Technol.*)

Conference Papers

1. <u>Lung-Sheng Lee</u> and Kuochen Wang "A Network Assisted Fast Handover Scheme for IEEE 802.16e Networks," in *Proceedings of the 18th IEEE International Symposium on Personal, Indoor and Mobile Radio Communications,* pp. 1-5, Sept. 2007.

2. Da-Ren Guo, Kuochen Wang and <u>Lung-Sheng Lee</u>, "Efficient Spatial Reuse in Multi-Radio, Multi-Hop Wireless Mesh Networks," in *Proceedings of the IEEE Vehicular Technology Conference*, pp. 1076-1080, April 2007.

3. Po-Hsiang Kang, Kuochen Wang, Hung-Cheng Shih, <u>Lung-Sheng Lee</u>, "Performance Enhancements of the EDCA in IEEE 802.11e Wireless LANs," in *Proceedings of the National Symposium on Telecommunications,* vol. 2, pp. 704-709, 2006.

4. Ping-Chi Wang, Kuochen Wang and <u>Lung-Sheng Lee</u>, "A QoS Scheme for Digital Home Applications in IEEE 802.11e Wireless LANs," in *Proceedings of the 16th IEEE International Symposium on Personal, Indoor and Mobile Radio Communications*, vol. 3, pp. 1845-1849, Sept. 2005.

5. C.K. Chen, Kuochen Wang, and <u>Lung-Sheng Lee</u>, "A Hybrid Overlay Multicast Routing Protocol for Mobile Ad Hoc Networks," in *Proceedings of the International Conference on Wireless Networks, Communications, and Mobile Computing*, Vol. 1, pp. 784-789, June 2005.

6. Kuochen Wang and <u>Lon-Sheng Lee</u>, "An Efficient QoS Supported Handover in Micro-Cellular ATM Networks," in *Proceedings of the 3rd Workshop on Mobile Computing*, pp. 126-131, Mar. 1997.